THE UNIVERSITY OF ALBERTA

A MODEL STUDY OF AN ISOLATED NINE-SPOT

by

W.E. CULHAM

SUBMITTED TO THE FACULTY OF GRADUATE STUDIES
IN PARTIAL FULFILMENT OF THE REQUIREMENTS FOR THE DEGREE
OF MASTER OF SCIENCE IN PETROLEUM ENGINEERING

DEPARTMENT OF CHEMICAL AND PETROLEUM ENGINEERING

EDMONTON, ALBERTA

OCTOBER 1962

ABSTRACT

In analyzing secondary recovery projects, the fraction of the reservoir which is ultimately swept by the injected fluid is of paramount importance. Treatment of water flood behavior, and in particular areal sweep efficiency, can best be studied by scaled flow model experiments.

In the displacement of oil by water in these two-dimensional flow systems capillary forces exhibit considerable influence. Laboratory results can only be utilized for field evaluations when capillary effects are overcome. A study conducted to determine the exact effect of these capillary forces disclosed that for sufficiently high injection rates the flooding behavior became independent of these forces and was considered stabilized.

Data was obtained on the performance of an isolated nine-spot waterflood. A general nine-spot correlation for areal sweep efficiency as a function of water injected was obtained for a wide range of mobility ratios. High oil recoveries and sweep out patterns were obtained for all mobility ratios studied.

ACKNOWLEDGEMENTS

The writer wishes to express his appreciation to D.L. Flock, Department of Chemical and Petroleum Engineering, University of Alberta, under whose direction this research project was carried out.

Thanks are also expressed to the technical staff of the Chemical and Petroleum Engineering shop for their assistance in design and construction of the equipment. The writer also wishes to thank his friends and colleagues for their helpful suggestions.

In addition the financial assistance of the Alberta Research Council is gratefully acknowledged.

TABLE OF CONTENTS

LIST OF TABLES

LIST OF FIGURES

INTRODUCTION

The objective of this research project was to obtain data on the performance of an isolated nine-spot flood. In particular the effect of mobility on oil recovery and areal sweep efficiency after water breakthrough was examined. Of secondary importance was an investigation to determine the relationship between water injection rate and the oil recovery.

A water flood normally consists of an array of identical well patterns. In such an array, the perimeters of the well patterns are axes of symmetry and act as impermeable boundaries. Thus, an extensive pattern water flood can be visualized as an aggregation of "confined" floods. In contrast, an isolated or pilot water flood involves only one pattern and is "unconfined". In this case the well pattern is not balanced by other flood units; hence the perimeter of the pilot area does not act as an effective boundary. This causes the amounts of oil and water produced in an isolated pattern to be different from that produced in an extensive flood.

The isolated water flood is the type of system under investigation in the subject report. The pattern studied was the nine-spot. This is a unit of nine wells on a square pattern. Producing wells are located at each corner of the square and midway along each side, with the injection well located at the centre of the square pattern.

Much research has been done on confined patterns of all types but little published work is available on isolated systems and in particular the isolated nine-spot pattern. One of the main purposes of

an isolated or pilot water flood is to obtain advance knowledge about the performance of a large scale water flood development. Therefore the difference in behavior of a confined and unconfined system should be known.

The work presented is based of flow model experiments. One model was employed for the entire study. It consisted of a maximum density sand bed, packed between two transparent lucite sheets. The flood front was visually observed by using a fluorescent tracer dye and three ultraviolet lamps. Distilled water was used as the displacing phase and several different viscosity oils were used as the displaced phase.

FUNDAMENTAL MODEL PROPERTIES

CAPILLARY PRESSURE

Capillary forces in a porous medium are the results of the combined effect of surface and interfacial liquid tensions, pore size and shape, and the wetting properties of the reservoir rock.[19] Capillary pressure can be described as a measure of the tendency of the rock to imbibe the wetting fluid phase or to repel the non-wetting phase.

The displacement of one fluid by another in the pores of a porous medium is either aided or opposed by the surface forces of capillary pressure.[6] As a consequence, in order to maintain a porous medium partially saturated with non-wetting fluid, while the medium is also exposed to wetting fluid, it is necessary to maintain the pressure of the non-wetting fluid at a value greater than that in the wetting fluid. Denoting the pressure in the wetting fluid by P_w and that in the non-wetting fluid by P_{nw}, we have

$$P_{nw} - P_w = P_c\,(S_w) \tag{1}$$

This is the defining equation for capillary pressure in a porous medium.

The fact that the capillary pressure-saturation curves of nearly all naturally occurring porous materials have many features in common has led to attempts to devise some general equation describing all such curves. Leverett[14] by utilizing dimensional analysis proposed the following relation,

$$J(S_w) = \frac{P_c}{\sigma \cos \theta}\sqrt{\frac{K}{\phi}} \tag{2}$$

where P_c = capillary pressure - dyne/cm^2

σ = interfacial tension - dyne/cm

K = permeability - cm^2

ϕ = fractional porosity

θ = contact angle

This J-function was originally proposed as a universal correlation for all porous media. However, subsequent work disclosed that it was only useful in correlating data connected with unconsolidated sands.

The evaluation of the capillary pressure versus saturation relation for the unconsolidated Ottawa sand (ASTM Designation C-109) system was carried out by Pritchard[20]. He used a lucite tube fitted with screen electrodes throughout its length and packed with Ottawa sand. A capillary pressure drainage curve was obtained and converted into Leverett's J-function. The results are plotted in figure 1.

ABSOLUTE, EFFECTIVE AND RELATIVE PERMEABILITY

Permeability is that property of a porous material which characterizes the ease with which a fluid may be made to flow through the material by an applied pressure gradient. Permeability is the fluid conductivity of the porous material.

Permeability is defined mathematically by Darcy's Law:

$$K = \frac{Q\mu L}{A(\Delta P)} \tag{3}$$

where K = permeability in darcies

Q = flow rate in cc/sec

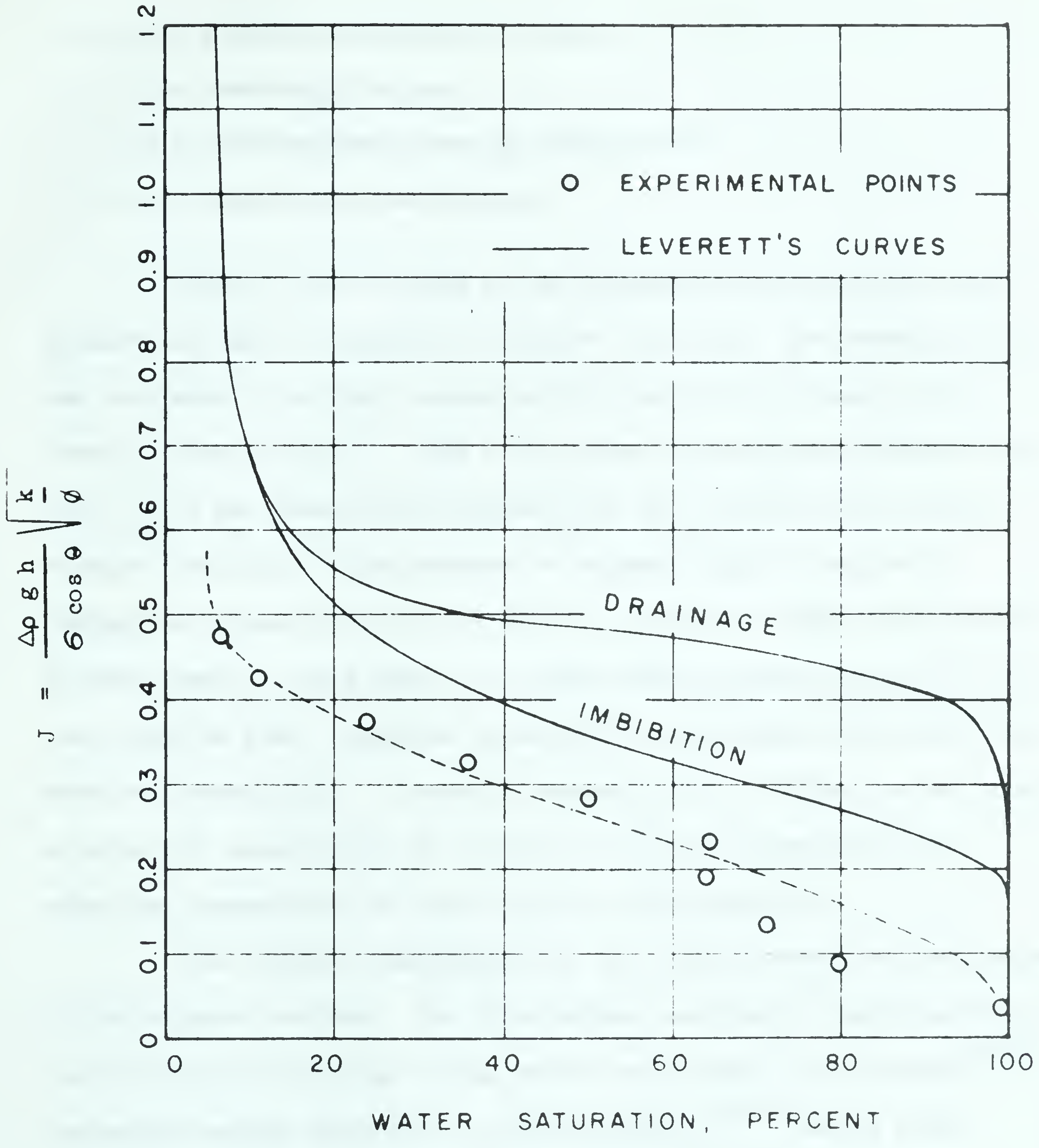

FIG. 1 CAPILLARY PRESSURE RESULTS COMPARED TO LEVERETT'S J-FUNCTION (AFTER PRITCHARD)

ΔP = pressure differential in atm.

L = core length in cm.

A = cross-sectional area of core in cm^2

μ = viscosity in centipoises

Darcy's Law is based on the assumption that only one fluid is present and that it completely saturates the rock. The permeability of the rock when it is fully saturated with one fluid is known as the "absolute permeability". When a fluid does not completely saturate the rock, as is the case in multi-phase flow, the ability of the rock to conduct that fluid in the presence of another fluid is called its "effective peremability" to the fluid in question. Since the presence of more than one fluid phase in a porous medium reduces the ability of each fluid to flow, effective permeabilities are always lower than the absolute permeability. "Relative permeability" is defined as the ratio of effective permeability to a fluid at a given saturation to the effective permeability to that fluid at 100% saturation.

The absolute permeability of the subject system was determined by two separate methods. The first method consisted of applying Darcy's Law to fluid flow through a sand packed lucite tube (See Pritchard[20]). The second method consisted of applying Muskat's[16] steady state, radial flow equation for a five-spot pattern to single fluid flow through the two-dimensional model. The calculations for the latter method are presented as Table 1 in Appendix A.

Pritchard[20] obtained effective and relative permeability data for the Ottawa sand by employing a steady state, desaturation

procedure. This method consists of introducing two fluids simultaneously into a linear system at a predetermined fluid ratio. The two fluids are injected through the core until steady state flow conditions are obtained and the existing saturations are stable. The saturations are determined by maintaining a volumetric balance of all fluids injected and produced. Once the saturation has been determined, the effective permeability of the two phases can be calculated by applying Darcy's Law to each phase individually. The effective permeabilities are present in Figure 2 and the relative permeabilities, as a ratio to the absolute permeability, are presented in Figure 3.

POROSITY

Porosity (effective) of a porous material is the fraction of the bulk volume occupied by interconnected voids.

The effective porosity of the model under study was determined by a simple material balance technique. The bulk volume of the model was calculated from the inside dimensions of the model. The model, containing dry sand, was saturated with water under vacuum and consequently all the pore spaces became completely filled with water (ie: one-hundred percent saturated with water). Thus by dividing the volume of the saturating fluid by the bulk volume the porosity was determined.

WETTABILITY

Rock surfaces can vary in their wettability, some being oil-wet and others water-wet. This factor of wettability enters into reservoir performance and also plays a primary role in laboratory investigations.

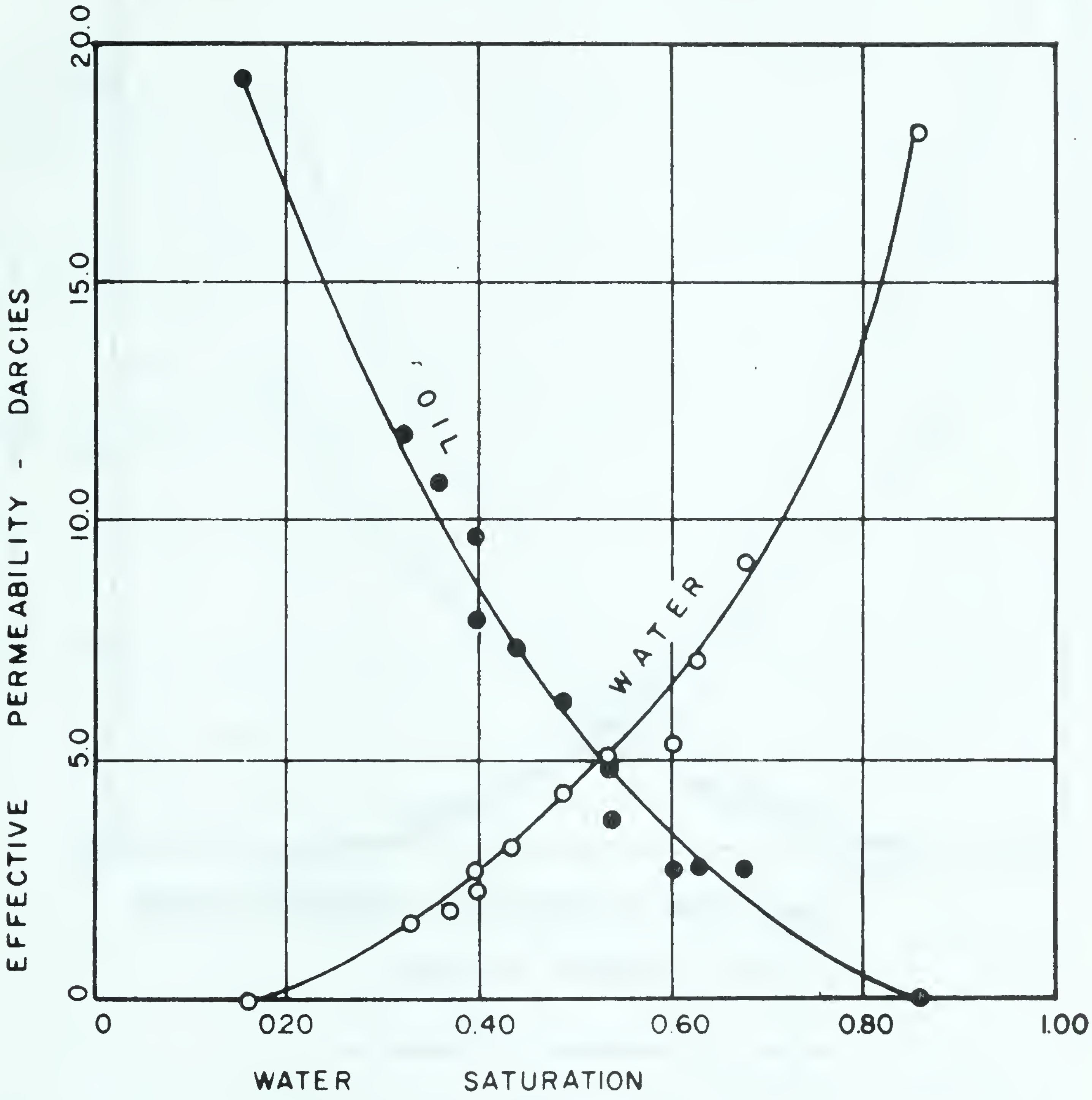

FIG. 2 EXPERIMENTAL EFFECTIVE PERMEABILITY CURVES (AFTER PRITCHARD)

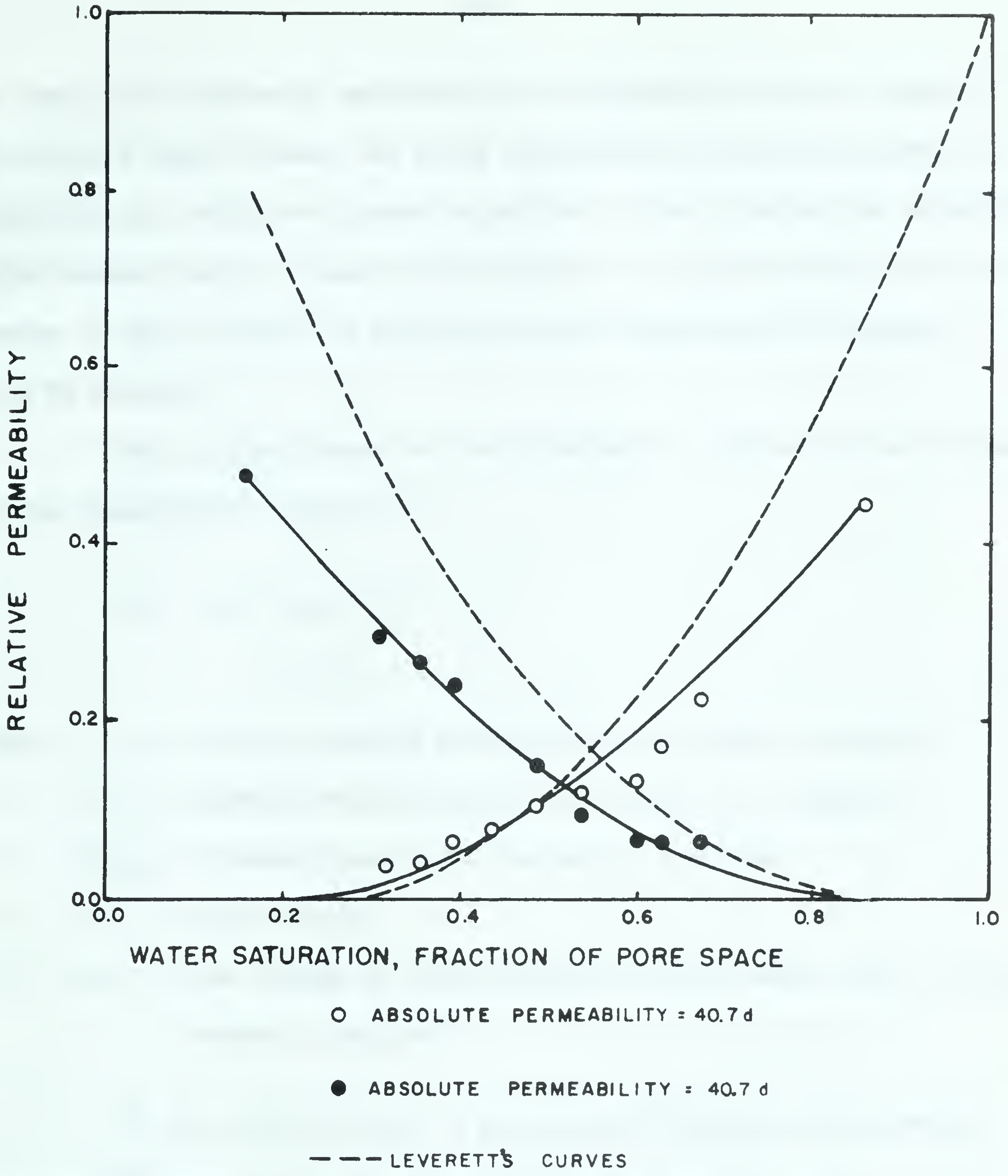

FIGURE 3 RELATIVE PERMEABILITIES
(AFTER PRITCHARD)

In theory, the degree of wettability is frequently defined in terms of the contact angle between the fluid interface and the solid surface. A preferentially water-wet system is defined as one in which the advancing water contact angle is less than 90 degrees. A preferentially oil-wet system is one in which the advancing water contact angle is greater than 90 degrees.

The surface forces in a solid-water-oil system can be related by the Young-Dupree equation[1]:

$$A_{sw} - A_{so} = \sigma_{ow} \cos \theta$$
$$= - \Delta F \qquad (4)$$

where: A_{sw} = adhesion tension between solid and water - ergs/cm^2

A_{so} = adhesion tension between solid and oil - ergs/cm^2

σ_{ow} = oil-water interfacial tension - dynes/cm

θ = contact angle

ΔF = free energy of displacement of oil by water from a solid surface - ergs/cm^2

If the contact angle is less than 90 degrees, the adhesion tension difference is positive and oil displacement by water from a solid surface will be spontaneous and favored by a high oil-water interfacial tension. If the angle is greater than 90 degrees the displacement will not be spontaneous but will require less energy the lower the oil-water interfacial tension. This behavior has been verified experimentally by Newcombe.[18]

To ensure that the sand used in the subject study was preferentially water-wet, it was washed with concentrated chromic acid and fired at 1100°F for 12 hours. To verify that this technique produced a water-wet sand a procedure suggested by Bobek[2] was employed.

Imbibition tests conducted on the Ottawa sand, using a volumetric apparatus identical to that used by Bobek, resulted in oil being spontaneously displaced from the sand by water. A plot of the volume of water imbibed versus time is presented as Figure 4. The reverse procedure of saturating the sand with water and having the oil act as the displacing phase resulted in no displacement. This latter test gave added assurance that the sand was definitely water-wet.

Figure 4 presents two curves which show the rate of imbibition for both the untreated and treated sand. The tests indicate that the imbibition process was more complete for the treated sand than for the untreated sand (ie: 86% to 76%). This indicates that the acid wash and heat treatment produced a more water-wet sand.

It should also be pointed out that the spontaneous displacement of oil by water from the treated sand would only occur after the treated sand was submerged in water for an extended period, dryed at room temperature and then saturated with oil. In addition the water used in the tests had to be slightly acidic. This was accomplished by adding a small amount of hydrochloric acid. Tests conducted on the treated sand immediately after the heat treatment resulted in only a small amount of water being imbibed (ie: less than 1% of the pore volume).

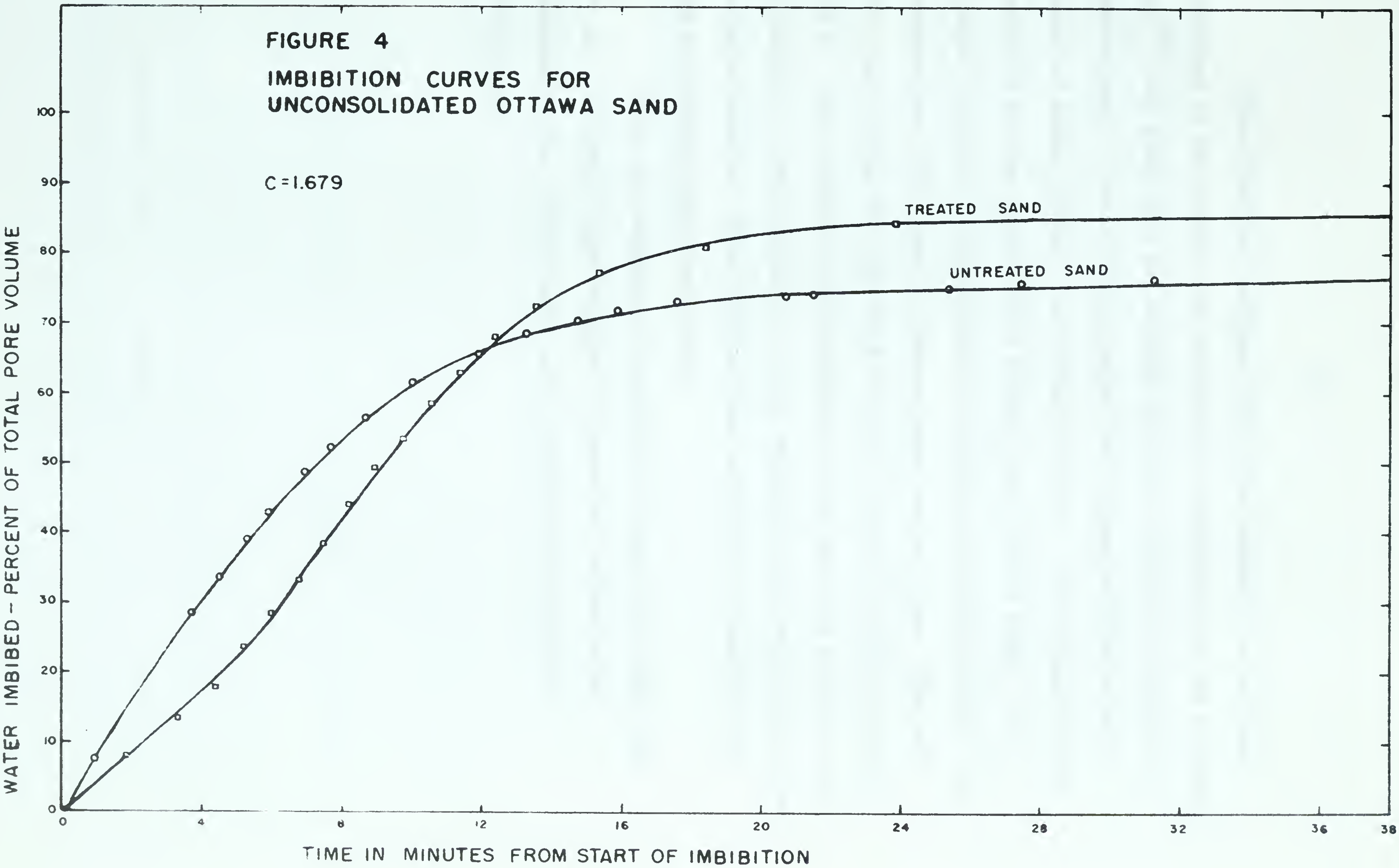

FIGURE 4

IMBIBITION CURVES FOR UNCONSOLIDATED OTTAWA SAND

These limiting conditions which were necessary to initiate imbibition in the treated sand tests might be attributed to the following. Weyl[26] has shown that the surfaces of glass, silica, etc. consist of hydroxy-groups. These hydroxy-groups extend hydrogen bonds to such liquids as water, glycerol and sulfuric acid as a result these liquids completely wet the material thus giving a zero contact angle. It is believed that the treated sand was so completely dehydrated by the heat treatment that this layer of hydroxy-groups was destroyed. Thus with this layer missing the sand would be wet by the first liquid in contact with it. This proposal is substantiated by the fact that after the sand was exposed to water and dried at room temperature the imbibition process was again possible. This indicated that imbibition is possible only when the hydroxy-groups are present.

Since the sandpack was initially in contact with water and not oil, the treated sand retained its water-wet preference and consequently the ensuing tests were conducted in a water-wet porous media.

MODEL STUDIES

One model was used for the entire series of floods, however due to difficulties encountered in changing oils two separate sand packs were necessary. Reservoir properties of each pack and model dimensions are included in Table 2 in Appendix A. The flood front during each flood was visually observed by using a water soluble fluorescent tracer dye excited by ultraviolet light.

Data taken during each run consisted of water injected, oil and water produced and producing water-oil ratio. In addition the area contacted by the injected water was traced on the top of the model. The pattern was later photographed and the area found by planimetering.

DESCRIPTION OF APPARATUS

The model was a maximum density sand bed packed between two transparent lucite sheets. The maximum density pack was obtained by bolting the model to a "Syntron" electric vibrator (Model VP - 60), fitted with a wooden top, and vibrating the entire model for ten hours.

A schematic diagram (Figure 5) shows the pattern of injection and producing wells. In addition to Figure 5 a photograph of the entire apparatus, including the lighting arrangement, is presented in Figure 6.

Nine simulated oil wells are located on an isolated pattern. There are also wells in the four outside corners of the model. Injection was maintained by means of a constant rate Ruska pump. A liquid filled mercury manometer fitted to the injection line served as a pressure

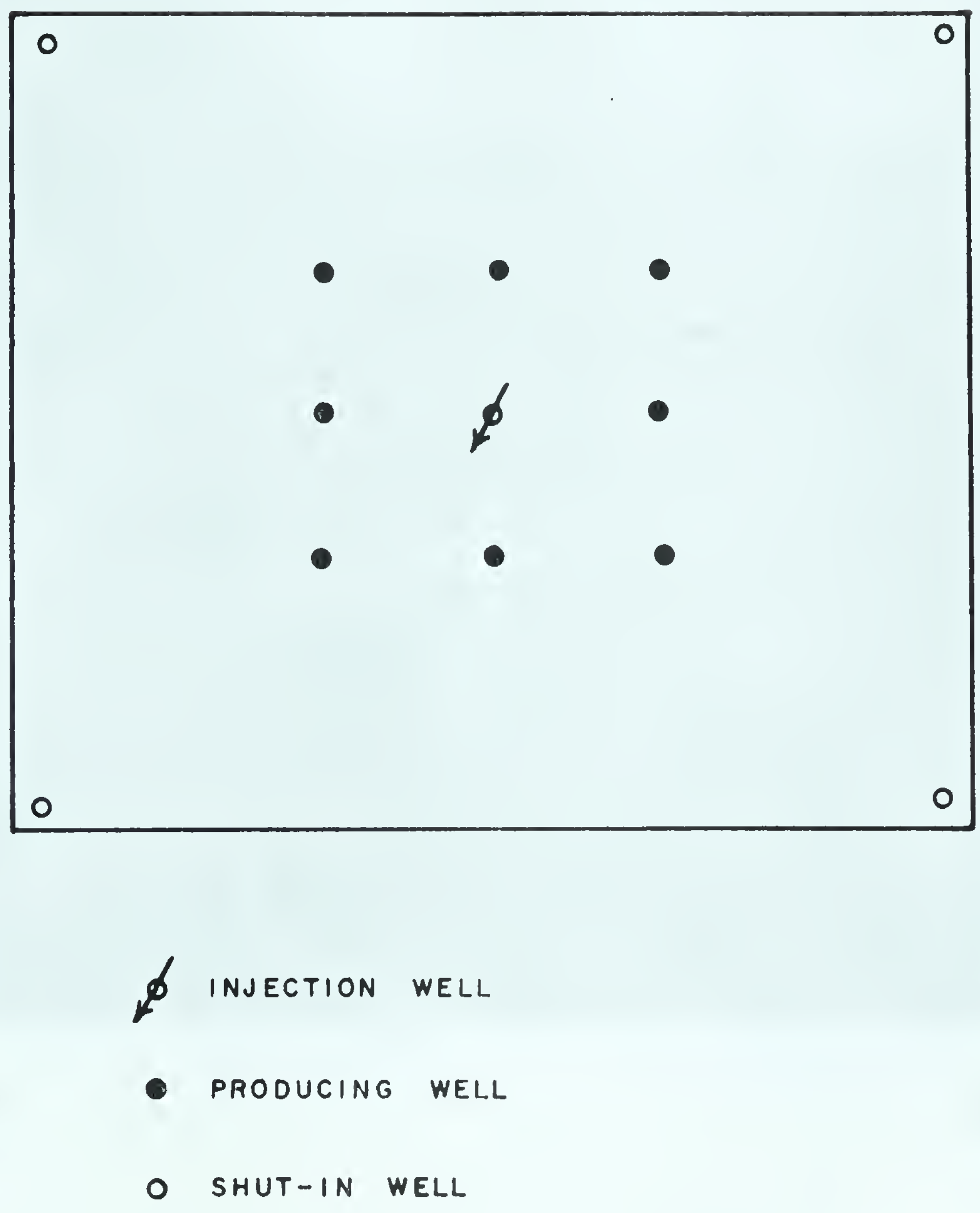

FIGURE 5

SCHEMATIC DIAGRAM OF ISOLATED NINE-SPOT WELL PATTERN

FIGURE 6. PHOTOGRAPH OF EQUIPMENT SHOWING TWO-DIMENSIONAL MODEL, INJECTION PUMP AND LIGHTING ARRANGEMENT.

measuring device. The producing wells discharged against a constant back pressure (See Figure 6) maintained by an elevated outlet flow line.

By using a highly efficient water soluble fluorescent tracer dye (C.I.L. - LTS) it was possible to trace the pattern covered by the injected water. The fluorescent dye, dissolved in the injection water, was made to fluoresce by being exposed to light emitted by three, 40 watt, ultraviolet lights which were closely fitted under the model. The fluorescent water could be easily traced by illuminating the bottom of the model with ultraviolet light in a dark room.

EXPERIMENTAL PROCEDURE

The bed was initially evacuated from the four corner wells and saturated with water from the centre well. By measuring the amount of water required to fully saturate the bed the porosity was calculated (see porosity section). The initial connate water saturation was established by flooding the water saturated bed with oil until no water was produced. After each flood the connate water was re-established by the same procedure. Six floods using fluids with different viscosity ratios were employed. The water viscosity was altered by adding glycerol. Oil and water viscosities were measured using Oswald viscometers. Interfacial tensions were measured with a Du Nory Tensiometer. All fluid properties are summarized in Table 3 (see Appendix A).

In resaturating the model with a different oil, the saturation was always carried out with a more viscous oil displacing a less viscous oil. To ensure that the model was fully saturated with the

new oil, the viscosity of the effluent oil was measured and if it was the same as the viscosity prior to injection the model was considered fully saturated.

As previously stated a record was kept of water injected, water and oil produced and producing water-oil ratio during each flood. All floods were terminated when approximately 25 pore volumes of water had been injected. In all cases the terminating water oil ratio was greater than ten to one.

The location of the flood front during each flood was recorded by contouring the top of the model. Injection was temporarily terminated each time the location of the flood front was traced.

After each flood was completed a photograph of the entire flood pattern was taken. A typical flood pattern is illustrated in Figure 7. By enlarging the photograph of each flood the area contacted by the injected water was found by using a planimeter.

DEFINITION OF TERMS AND CALCULATION PROCEDURES

Definitions

Many of the fundamental properties that must be known to determine the merits of a secondary recovery operation can be evaluated by core analysis or linear flood investigation. However, to fully evaluate a secondary recovery project such information as area sweep efficiency, vertical sweep efficiency and total sweep efficiency must be evaluated. This can be done by using a three-dimensional model.

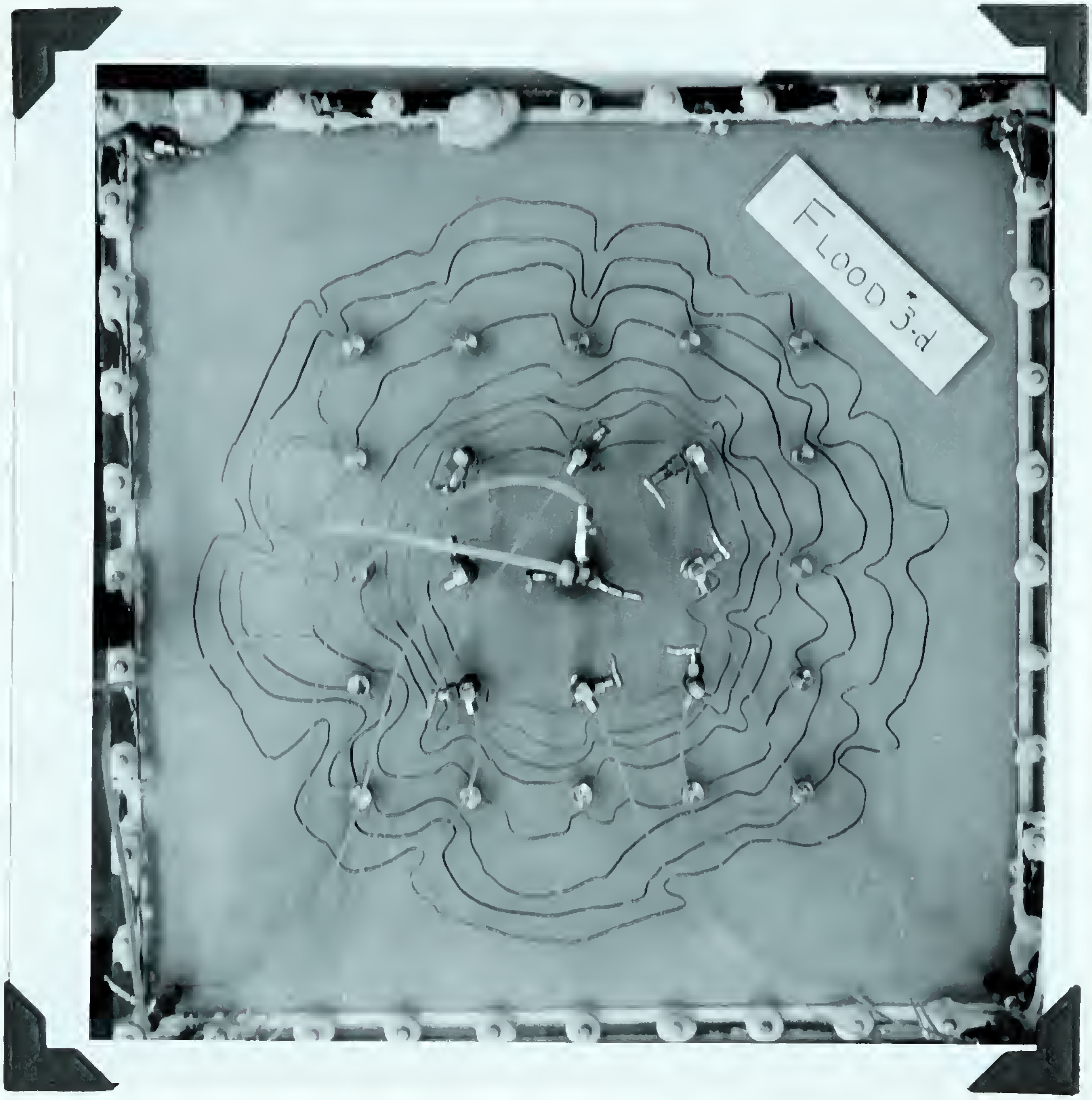

FIGURE 7. PHOTOGRAPH OF FLOOD 3-d ILLUSTRATING THE LOCATION OF THE FLOOD FRONT DURING VARIOUS STAGES OF INJECTION.

It has been found that the amount of recoverable oil can be determined by water flooding small core samples. When the amount of recoverable oil is expressed as a fraction of the pore volume, it is called the "displacement efficiency" to a water flood for that particular rock. Multiplying this displacement efficiency, for a particular sample, by the total pore volume of the hydrocarbon bearing rock will give the maximum possible recovery of oil by a water flood. This however, is only half the information required to calculate the expected oil recovery of a pattern flood. In addition to knowing the displacment efficiency, it is also necessary to be able to predict the areal fraction of the reservoir which will be invaded by water. By combining these two factors oil production can be calculated as follows:

$$\text{Oil Recovery} = E_d \times E_{as} \times P.V._{res} \qquad (5)$$

where E_d is the displacement efficiency, E_{as} is the areal sweep efficiency and $P.V._{res}$ is the total pore volume of the oil reservoir (unit area). By dividing by $P.V._{res}$ the following relation is obtained:

$$E_s = E_d \times E_{as} \qquad (6)$$

Here E_s is referred to as the total sweep efficiency. In actual fact the above relationships are not complete. The equations should also include a vertical sweep efficiency term. It is obvious that a non-homogeneous reservoir, such as one having strata of different permeability, will not be evenly or completely invaded on the vertical scale by the injected water. In the case of the sand packed reservoir the vertical sweep efficiency will be 100% due to its homogeneous nature. Consequently, the vertical term is not considered in the subject study.

The previous statements can be reiterated in the following brief definitions. Areal sweep efficiency is defined as the measure of the area of a reservoir which is contacted by the injected fluid at any time as compared to the unit area of the pattern. Displacement efficiency refers to the fraction of oil which is swept from the individual pores as compared with the amount of oil originally in place in the pores.

Many variables will affect the areal sweep efficiency of a water flood. The two factors exerting the most influence on the flood pattern were found to be the injection pattern and mobility ratio. Mobility can be thought of as a measure of the ease with which the fluid will flow through the rock. The mobility as used in this study is defined as:

$$M = \frac{\text{Displacing phase mobility}}{\text{Displaced phase mobility}} = \frac{K_W/\mu_W}{K_o/\mu_o} \quad \text{or}$$

$$M = \frac{K_W\mu_o}{K_o\mu_W} \tag{7}$$

where M is the fluid mobility; K_w, K_o are the effective permeability of the porous medium to water and to oil respectively and μ_w and μ_o are water and oil viscosities.

Calculation Procedures

All areal sweep efficiencies used in this report were obtained from direct measurement, as outlined in the previous section on experimental procedure. One exception to this is the areal sweep efficiency at

breakthrough. The breakthrough sweep efficiency values were calculated from:

$$E_s = E_{as} \times E_d \tag{6}$$

The total sweep efficiency (E_s) was calculated from the oil production at breakthrough. The displacement efficiency was also calculated and the procedure will be explained later. Thus knowing two terms of equation six the breakthrough efficiency was calculated.

All displacement efficiency terms referred to hereafter are calculated values. The displacement efficiency is simply the change in oil saturation in the swept zone. It is calculated by dividing the volume of oil recovered by the amount of oil originally in place in the zone swept by the injected fluid, up to the time in question. It is obvious that a saturation gradient exists from the injection well to the flood front and since there is no satisfactory method of determining this gradient, the calculated displacement efficiency must be regarded as representing an average value in the swept region.

The mobility ratios were calculated in the following manner:

1. The average saturation behind the flood front is obtained from the calculated displacement efficiency and the connate water saturation. Thus the saturation of the invading fluid behind the front is given by:

$$\overline{S}_w = S_{cw} + (1-S_{cw})E_d \tag{8}$$

where $\overline{S}_w$ is the average water saturation behind the flood front, S_{cw} is the connate water saturation and E_d is the average displacement efficiency.

2. The effective (or relative) permeability to water at this saturation is read from the experimental effective (or relative) permeability curves.

3. The effective (or relative) permeability to oil is the value corresponding to the oil saturation at the flood front. It there is no gas phase, as is the case in this study, this will be the connate water saturation.

4. The values are substituted along with the respective viscosities into the equation:

$$M = \frac{K_w \mu_o}{K_o \mu_w} \tag{7}$$

where all terms are as defined previously.

The stringent definition of mobility ratio is the summation of the mobility of each phase behind the flood front compared to the summation of the mobility of each phase ahead of the flood front. However, since the mobility ratio of the oil behind the flood front was small it was disregarded and since the connate water ahead of the front was considered immobile equation 7 is applicable.

LITERATURE REVIEW

Model Studies

Several methods have been devised to study the sweep efficiencies of an oil-water-porous media system. Early workers[13,27] found that it was possible to model actual reservoirs by using the analogy between fluid flow in a porous media and flow of an electric current through a resistance bed (potentiometric model) or the flow of ions through a

conducting solution (electrolytic model). The use of such models is based on the fact that voltage distribution in electric conductors can be represented by Laplace's equation, which also can be used to represent the pressure distribution of steady state, incompressible fluid flow in a homogeneous porous media. Pressure drops are equated to voltage drops; flow rates to current rates; and other parameters are equated to resistances.

Sweep efficiencies have also been studied with the techniques of applied mathematics. Muskat[5] has been the leading authority in this type of approach. However, even for simple systems the resulting mathematical equations are complex and difficult to solve.

Most of the above approaches are limited by the assumption that the invading and invaded fluids have the same flow properties (ie: unit mobility). Consequently dimensionally scaled models of reservoir elements, in which the properties of the rock and the fluids in the model are properly scaled to reservoir conditions, were introduced. Slobod and Caudle,[24] early workers in this field, introduced the X-ray shadowgraph model as a means of readily studying the effects of mobility on sweep efficiencies. The reservoir unit was a porous plate which was sealed on the top, bottom and edges. Variations in mobility ratios were obtained by varying the viscosity of the fluids. The injected fluid contained an X-ray absorbing material and the flood front was followed on a fluorescent screen or film.

Numerous papers outlining the effect of mobility ratio and other parameters on sweep efficiency have been published. Most of these papers only considered areal sweep efficiency up to breakthrough. Production after breakthrough was not considered.

Work by Dyes et al[9] has taken into account additional sweepout after breakthrough. The X-ray shadowgraph technique was used to determine the influence of fluid mobilities on the sweepout pattern when injection was extended to cover the producing period which followed breakthrough.

Craig, Geffen and Morse[7] investigated the effect mobility ratio and the volume of water injected had on areal sweep efficiencies in pattern floods after breakthrough. They found good agreement between their work and that of Dyes et al for areal sweep efficiency at breakthrough for various mobility ratios.

Although the above two investigations take into account the variation of areal sweep efficiency after breakthrough they were concerned with only pattern (confined) systems. Since pilot or unconfined patterns are often used to obtain advance knowledge about the performance of large scale water flood developments, the difference in behavior of confined and unconfined systems should be examined.

Neilson[17] investigated the performance of an isolated, inverted five-spot pattern at a constant mobility ratio. The study disclosed that areal sweep efficiencies of very high magnitude (ie: 600%) were obtained after breakthrough for a water oil ratio of 20:1.

Additional work by Caudle et al,[4,5] Dalton et al[8] tend to substantiate Neilson's work. These papers are also concerned with additional production and increased areal sweep efficiencies obtained from undrilled areas of an oil field. These studies employed artificial consolidated sand models. The results disclosed that considerable area

outside the normal well pattern was contacted by the injected fluid and consequently contributed to production.

Critical Rate

There are numerous published papers concerned with the effect of water injection rates on oil recovery. Various investigators[10,11,12 15,18,20,21] have shown that oil recovery increased, decreased or remained stabilized with increases in the rate of injected water.

Rapoport and Leas[21] found that for a linear water flood, recovery varied with length, rate and the viscosity of the displacing phases; for a given porous media and a given water-oil viscosity ratio. They also found that for floods with the same $Lv\mu_w$ product, the production behavior was similar, that is equal injection volumes resulted in equal recoveries. This resulted in their proposal of $Lv\mu_w$ as a general scaling coefficient for model tests. They further discovered that at some critical value of $Lv\mu_w$, recovery was independent of this factor; this is referred to as the critical scaling coefficient and thus "v" as the critical rate.

Separate studies by Newcombe[18] and Kyte[12] support Rapoport's investigation. That is oil recovery in linear systems (regardless of preferential wettability) increased with increasing rate up to a point where further increases in rate resulted in no additional recovery.

Investigations conducted by Jones-Parra[11] and Engleberts[10] disclosed that oil recovery decreased with increasing injection rates. However this reverse behavior was attributed to viscous fingering.

All of the previously mentioned investigations were primarily concerned with the scaling of linear flow systems and hence are somewhat limited. Consequently the formulation of more general scaling laws, applicable to three-dimensional systems, was necessary. Rapoport[22] has derived scaling laws applicable to three-dimensional systems. The laws were established on a mathematical basis and are applicable to incompressible immiscible, two phase flow systems. Particular consideration was placed on the roles of capillary pressure functions and relative permeability.

A laboratory investigation conducted by Rapoport[23] employs the previously mentioned scaling laws. Theoretical consideration, verified by experimental work, disclosed that areal flooding behavior depends specifically upon the rate of injection per unit sand thickness. More generally, it was seen that the displacement of oil by water in a two-dimensional flow system was largely governed by the dimensionless group of parameters;

$$C_2 = \frac{q\,\mu_w}{\sigma_{ow}\cos\theta\sqrt{K\phi}} \tag{9}$$

where q is injection rate per unit sand thickness, μ_w is water viscosity, σ_{ow} oil-water interfacial tension, K is permeability and ϕ is porosity. Derivation of the above equation is presented in Appendix B.

This group "C_2" was designated as the "capillary pressure coefficient" because its value defined the relative importance of capillary forces in the displacement of oil by water. It was found that for a given value of C_2 all porous media of given geometry, operated

under similar boundary conditions, and characterized by the same oil-water viscosity ratio, the same fractional flow, relative permeability and J-functions, will yield the same flooding behavior (ie: the same relation between water injection and oil production).

As was the case in linear systems, a critical value of C_2 existed. When this critical value was exceeded the two-dimensional water-oil displacements became independent of rate and were qualified as stabilized.

EXPERIMENTAL RESULTS AND DISCUSSIONS

CRITICAL RATE STUDY

Results

To ensure that the results obtained in this study would represent field behavior as close as possible, the influence that capillary pressure exerted on laboratory data had to be determined. To accomplish this a critical rate study was conducted. Two fluid systems of different viscosities were employed. The two systems are identified as follows:

Flood Series 3 - Oil-water viscosity ratio of 6.265

Flood Series 1 - Oil-water viscosity ratio of 1.679

Since a two-dimensional system was employed in the subject study it was expected that areal sweep efficiency, displacement efficiency and total sweep efficiency (oil recovery) would be influenced by capillary forces. To determine the magnitude of this effect, numerous floods were conducted on the two systems at different injection rates. Injection rates varied from 2.31 B/D/ft (320 cc/hr) to 20.20 B/D/ft (2800 cc/hr). The production history of flood Series 1 and 3 are given in tables 4 to 15 inclusive. Areal sweep efficiencies and calculation of displacement efficiencies for the subject series of floods are presented in Tables 20 to 30 inclusive. The basic information presented in the previously mentioned Tables are graphically represented in Figures 8 to 14 inclusive.

In figures 8 and 12 oil recovery has been plotted against Rapoport's[22] two-dimensional scaling coefficient. All terms in the

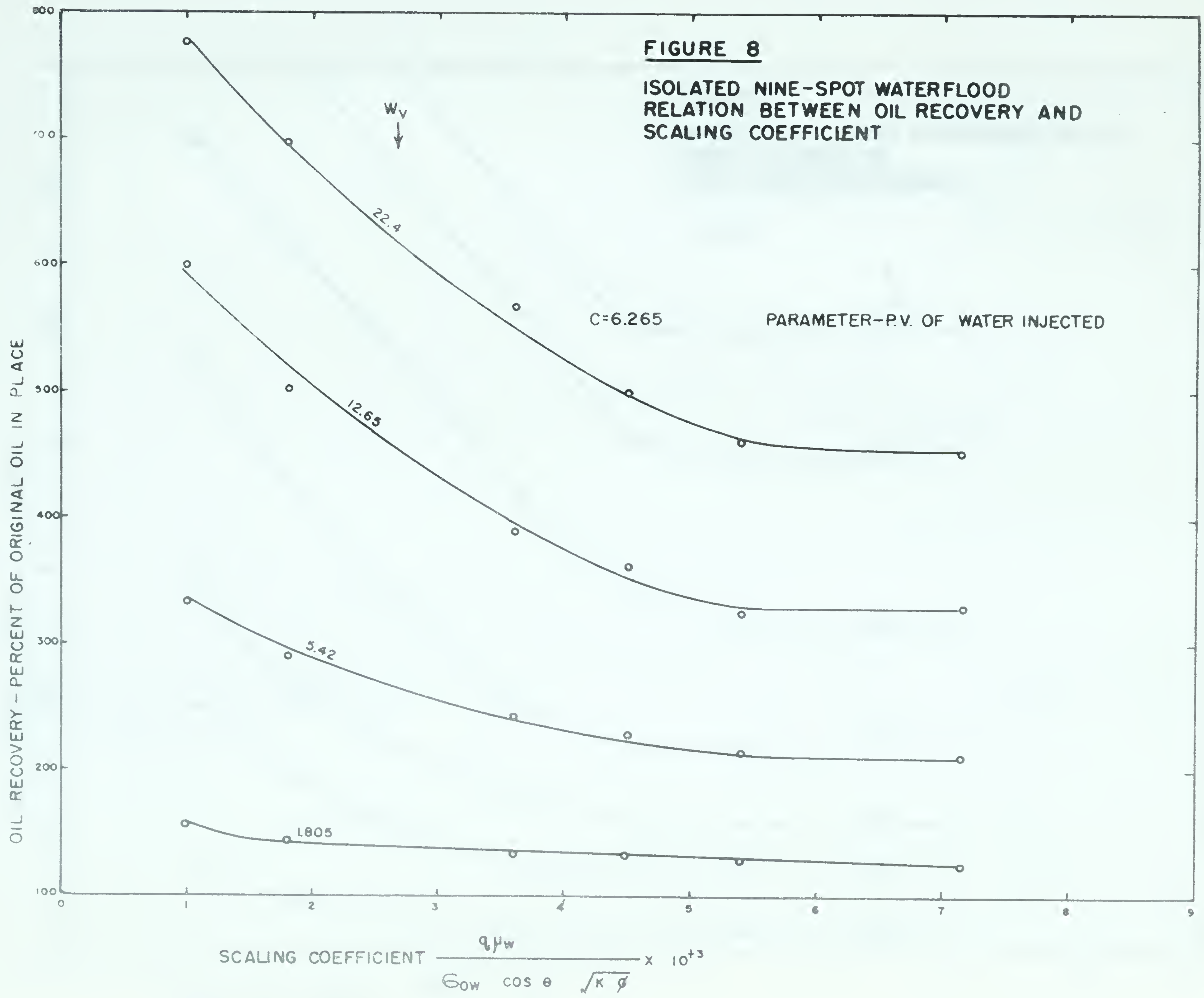
FIGURE 8
ISOLATED NINE-SPOT WATERFLOOD
RELATION BETWEEN OIL RECOVERY AND
SCALING COEFFICIENT
W_V
22.4
12.65
5.42
1.805
C=6.265
PARAMETER-P.V. OF WATER INJECTED
OIL RECOVERY - PERCENT OF ORIGINAL OIL IN PLACE
100
200
300
400
500
600
700
800
0
1
2
3
4
5
6
7
8
9
SCALING COEFFICIENT $\frac{q \mu_w}{\sigma_{ow} \cos\theta \sqrt{K \phi}} \times 10^{+3}$

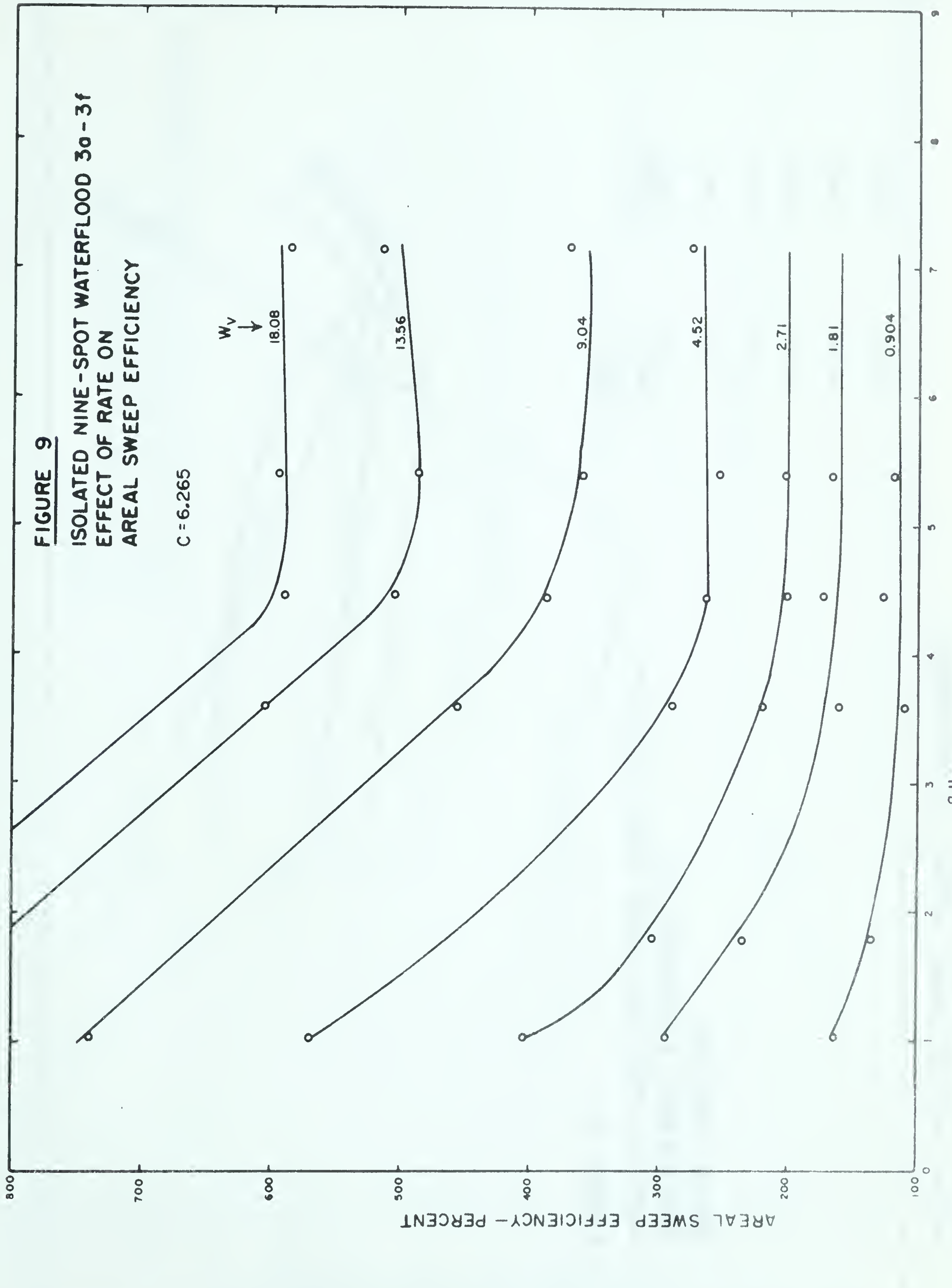

FIGURE 9
ISOLATED NINE-SPOT WATERFLOOD 3a - 3f
EFFECT OF RATE ON
AREAL SWEEP EFFICIENCY

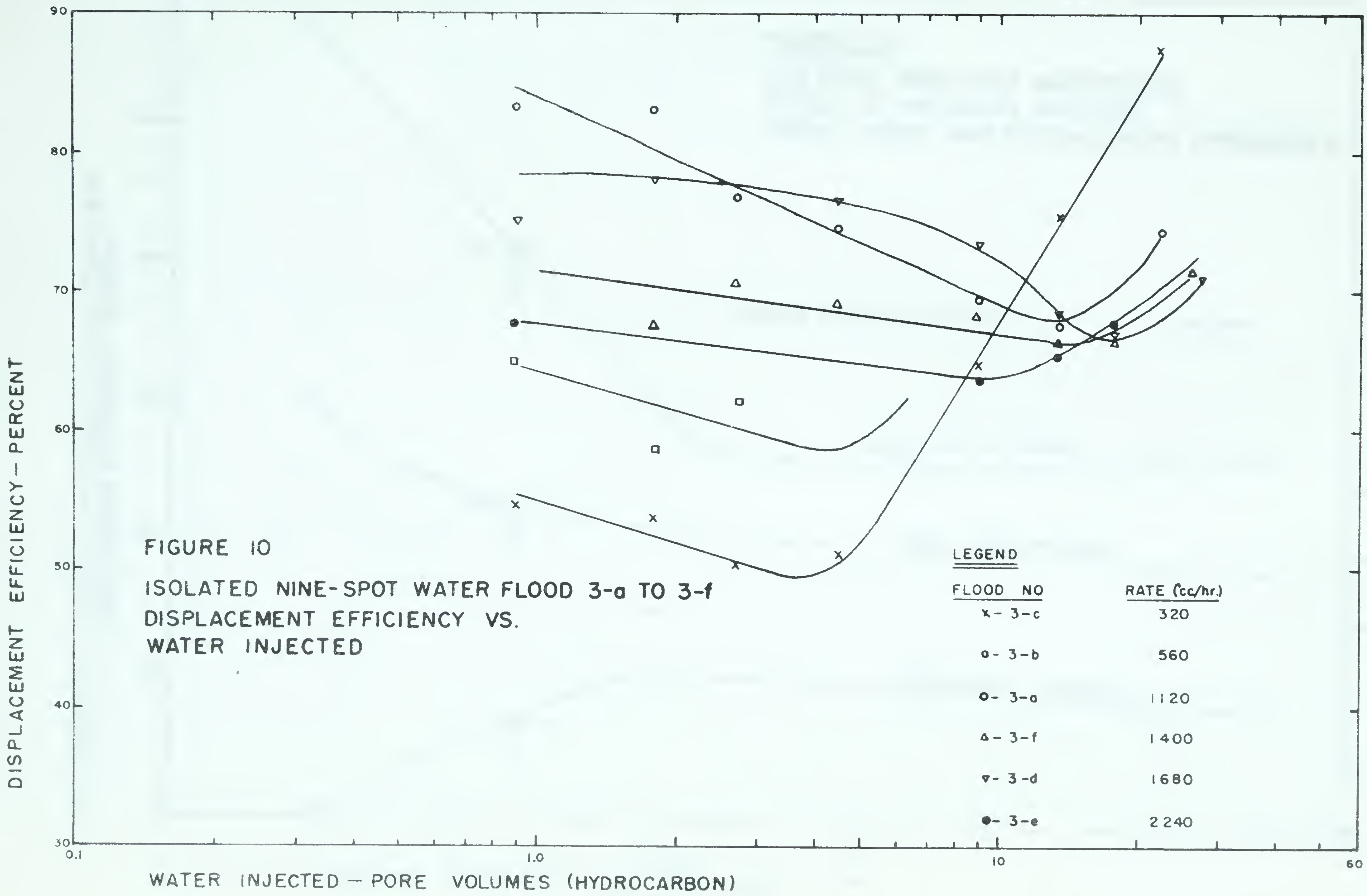

FIGURE 10

ISOLATED NINE-SPOT WATER FLOOD 3-a TO 3-f
DISPLACEMENT EFFICIENCY VS.
WATER INJECTED

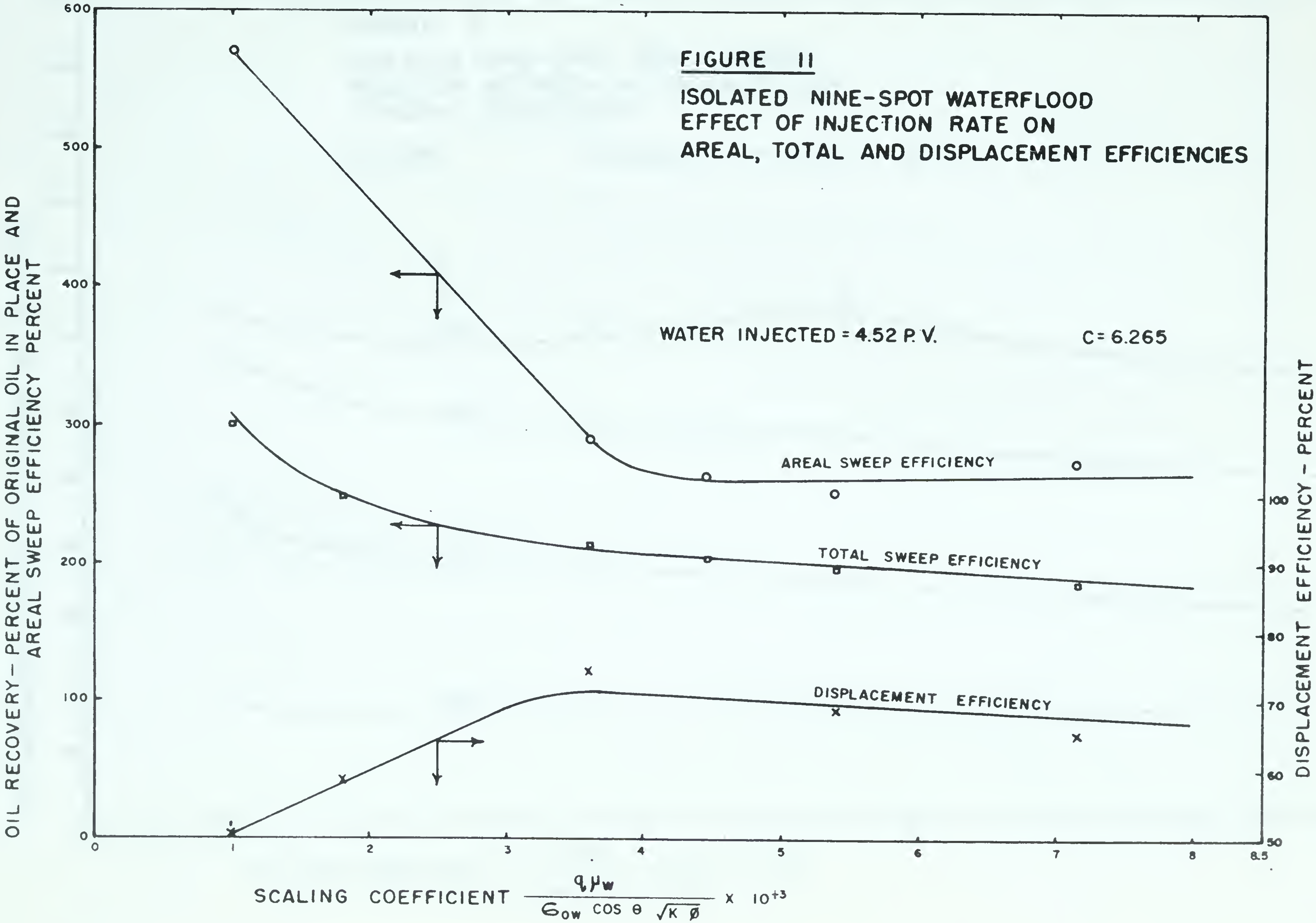

FIGURE 11
ISOLATED NINE-SPOT WATERFLOOD
EFFECT OF INJECTION RATE ON
AREAL, TOTAL AND DISPLACEMENT EFFICIENCIES
WATER INJECTED = 4.52 P.V.
C = 6.265
AREAL SWEEP EFFICIENCY
TOTAL SWEEP EFFICIENCY
DISPLACEMENT EFFICIENCY
OIL RECOVERY – PERCENT OF ORIGINAL OIL IN PLACE AND AREAL SWEEP EFFICIENCY PERCENT
DISPLACEMENT EFFICIENCY – PERCENT
SCALING COEFFICIENT $\frac{q \mu_w}{\sigma_{ow} \cos\theta \sqrt{K \phi}} \times 10^{+3}$
0
100
200
300
400
500
600
50
60
70
80
90
100
1
2
3
4
5
6
7
8
8.5

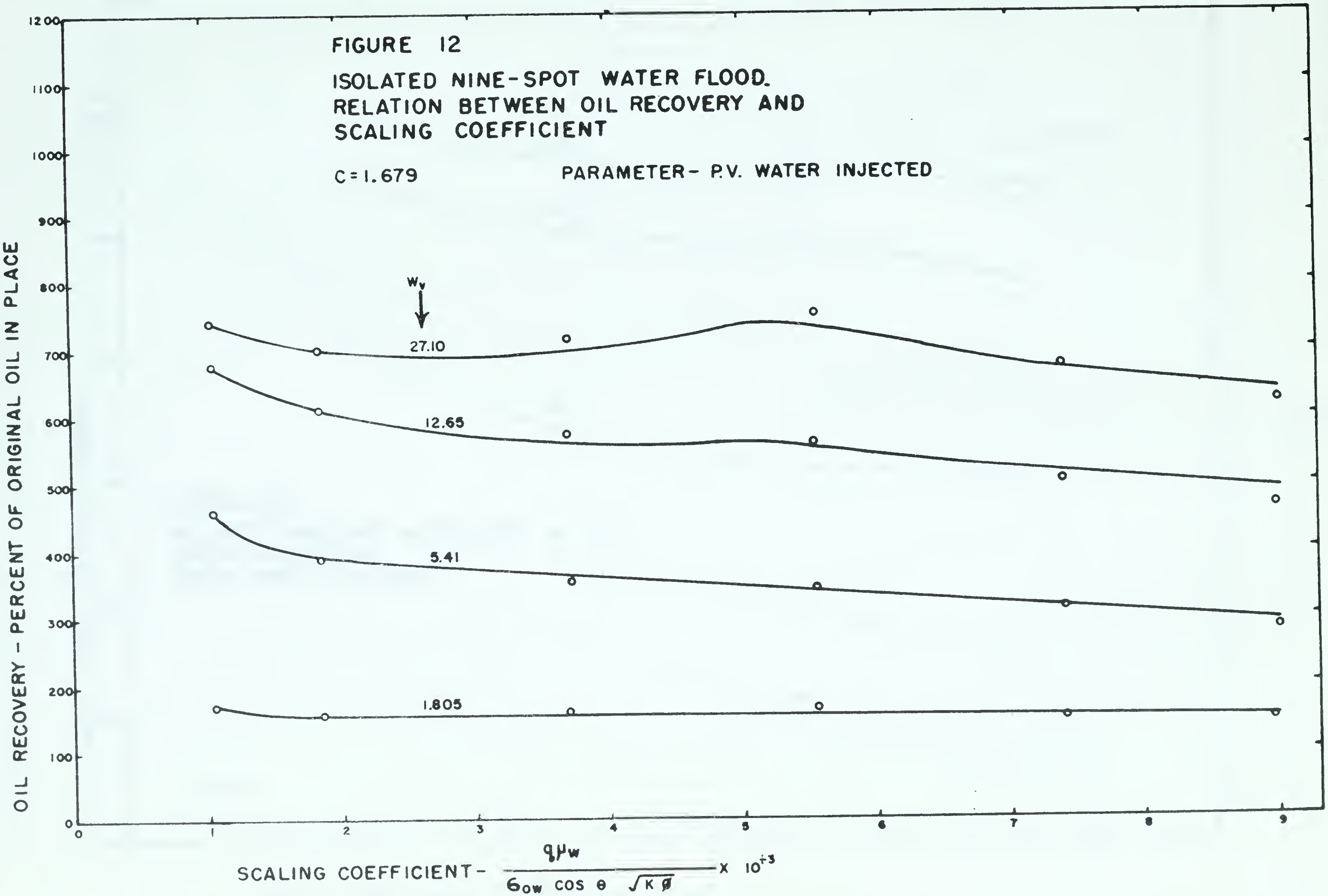

FIGURE 12

ISOLATED NINE-SPOT WATER FLOOD.
RELATION BETWEEN OIL RECOVERY AND SCALING COEFFICIENT

C = 1.679 PARAMETER - P.V. WATER INJECTED

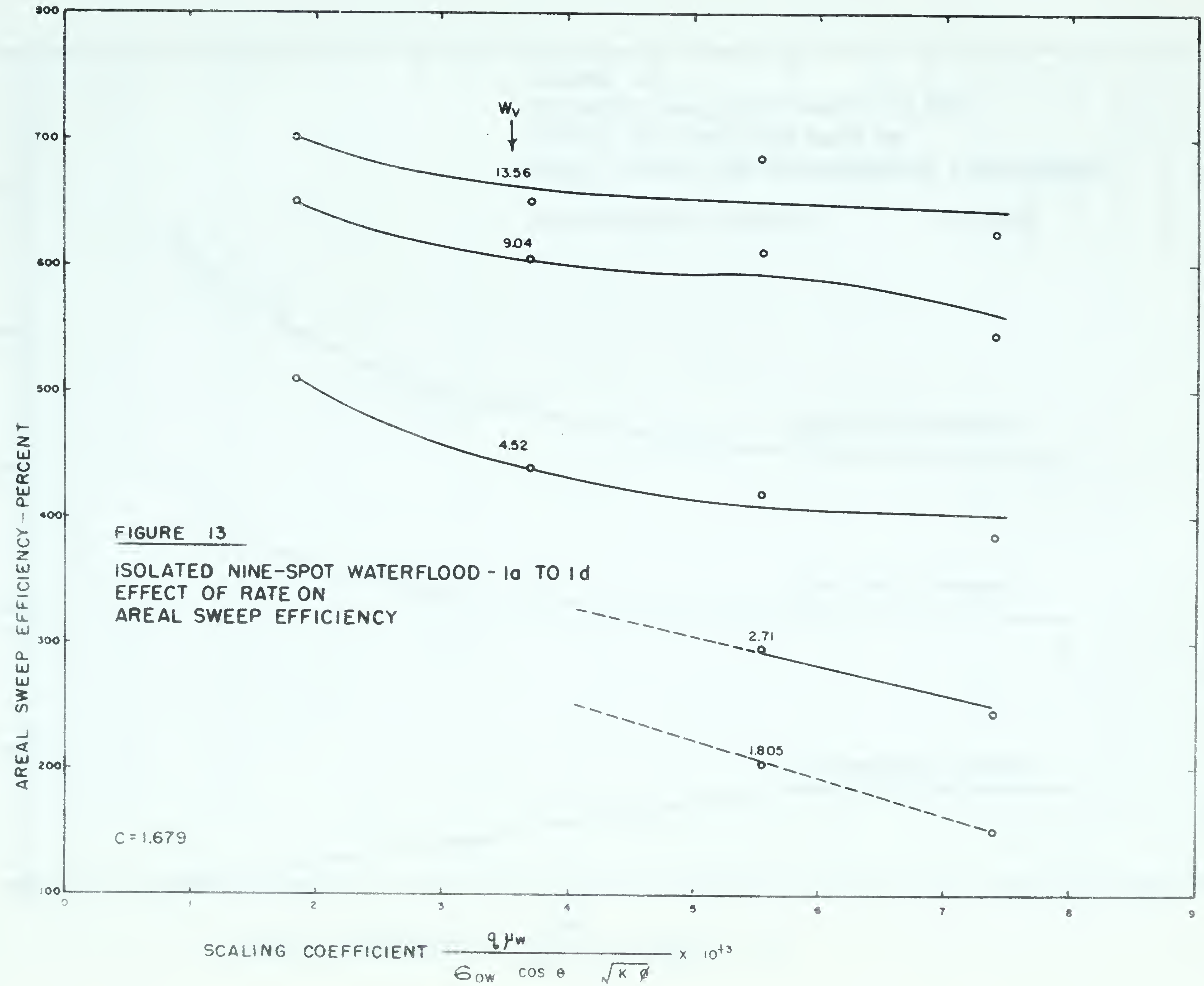

FIGURE 13

ISOLATED NINE-SPOT WATERFLOOD – Ia TO Id
EFFECT OF RATE ON
AREAL SWEEP EFFICIENCY

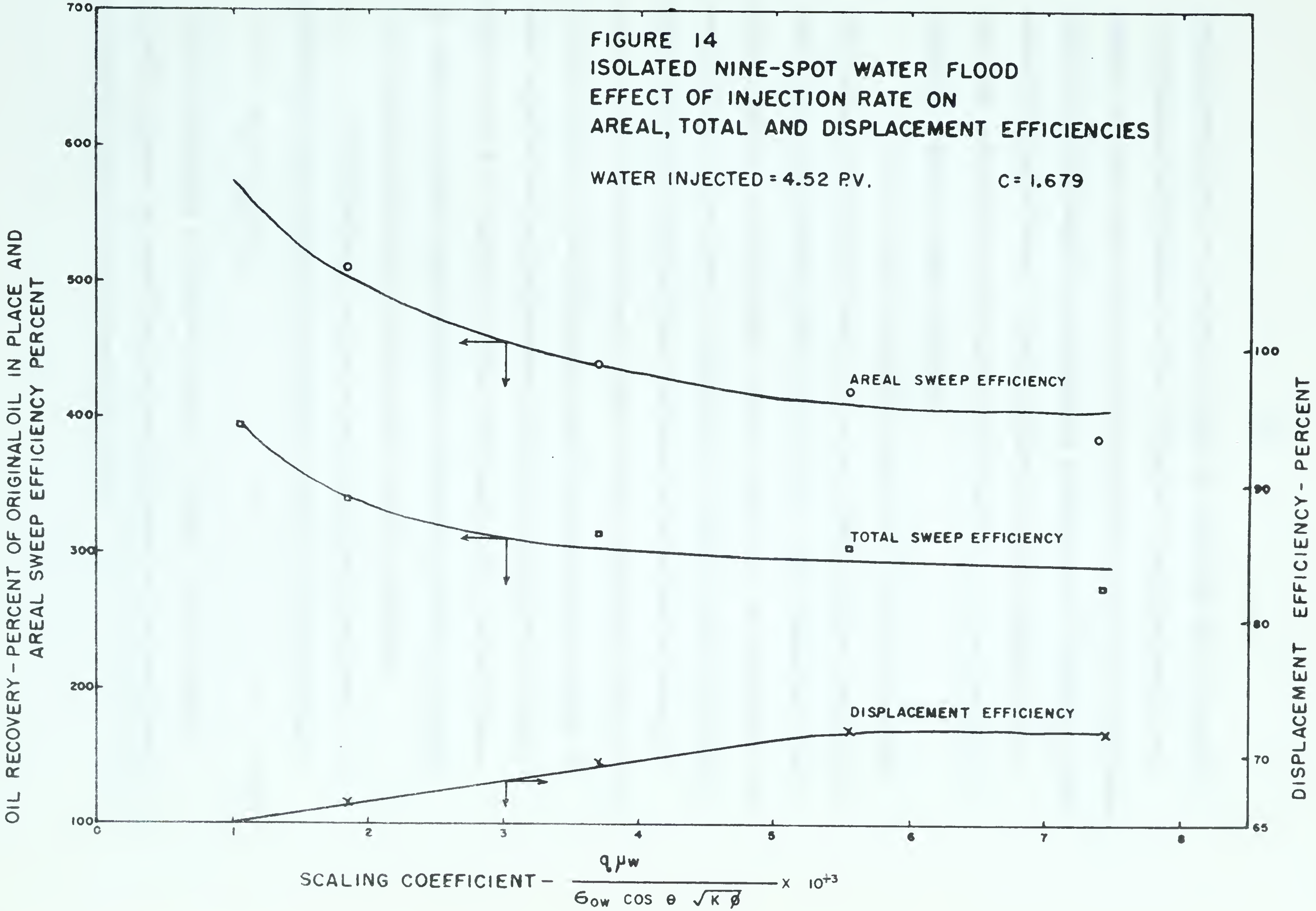
FIGURE 14
ISOLATED NINE-SPOT WATER FLOOD
EFFECT OF INJECTION RATE ON
AREAL, TOTAL AND DISPLACEMENT EFFICIENCIES
WATER INJECTED = 4.52 P.V.
C = 1.679
AREAL SWEEP EFFICIENCY
TOTAL SWEEP EFFICIENCY
DISPLACEMENT EFFICIENCY
OIL RECOVERY - PERCENT OF ORIGINAL OIL IN PLACE AND AREAL SWEEP EFFICIENCY PERCENT
DISPLACEMENT EFFICIENCY - PERCENT
SCALING COEFFICIENT - $\frac{q \mu_w}{\sigma_{ow} \cos \theta \sqrt{K \phi}} \times 10^{+3}$
700
600
500
400
300
200
100
0
1
2
3
4
5
6
7
8
100
90
80
70
65

scaling coefficient are constant except the injection rate, therefore, it represents only changes in rate. Figures 9 and 13 represent the changes in areal sweep efficiency with injection rate for the two floods. Figure 10 shows changes in displacement efficiency as a function of the volume of injected water. Finally, Figure 11 and 14 compare areal, total and displacement efficiencies as a function of injection rate at 4.52 pore volumes of water injected.

As can be seen from Figures 8 and 12 oil recovery decreases with increasing injection rate up to a point where further increases in rate do not significantly affect oil recovery. This phenomena is much more pronounced in flood Series 3 than in Series 1. An explanation for this will be offered later. Examination of figures 9 and 13 discloses that areal sweep efficiency also decreases with increasing rates of injection and then stabilizes. Again the most significant changes occur in Flood Series 3. The effect that injection rate and the volume of water injected has on displacement efficiency is depicted in Figure 10. Figures 11 and 14 compare all three efficiencies for the two floods. In these two figures the displacement efficiency is seen to increase with injection rate up to a certain point and then stabilize.

It is important to note at this point that the three efficiencies are related, as pointed out earlier, by the following:

$$E_s = E_{as} \times E_d \tag{6}$$

Further examination of Figures 11 and 14 indicate that the rate of injection appears to exert the greatest influence on the areal sweep efficiency, making it the controlling factor.

Discussion

In both series of floods employed to study the effect of rate on the behavior of water flooding, the displacement efficiency (E_d) followed a pattern which has been put forth by several authors.[12,18,21] That is the displacement efficiency increased with the rate of injection up to a point where further increases in rate caused no further significant changes. (See Figures 11 and 14).

In studies by Rapoport,[21] Newcombe[18] and Kyte,[12] conducted on linear systems, all authors found that oil recovery (oil recovery is equivalent to displacement efficiency in a linear system since the areal sweep is 100%), increased with increasing rate up to a point where further rate increases resulted in no additional recovery. This behavior was found to hold true for both preferentially oil-wet and water-wet systems, provided capillary end effects were absent.

This phenomena of increasing displacement efficiency (or oil recovery for linear systems) with increasing injection rates in water-wet systems may be explained by the tendency of water to imbibe into the smaller, tighter channels.[18] At low flood rates, flow channels are established by imbibition through the smaller channels.* At slightly higher rates more water pushes into larger channels as the flow capacity of the imbibition channels are exceeded. At still higher rates more injected water is carried by the larger channels with the result that

---

* At low rates it would appear at first that both large and small channels would be flooded. However if the rate of imbibition is as great or greater than the rate at which water is being injected then all the water would flow through the smaller channels by-passing large channels.

some oil is trapped and by-passed in the tight channels. The maximum displacement efficiency occurs then at the injection rate where water flows at the same rate of linear advance through both large and small channels. Hence an optimum rate occurs at which displacement efficiency is a maximum. This has been reported by Maguss,[15] Pritchard[20] and Jones-Parra.[11]

All literature is not in agreement with the above statements. Results of decreasing oil recovery (displacement efficiency) with increasing rates has been reported.[10,11] However, in all of these cases high oil-water viscosity ratios were involved. This behavior of decreasing displacement efficiency with increasing rate was attributed to fingering. Viscous fingering results from the situation that the inlet saturation distribution does not reach equilibrium at high rates. At low rates the capillary forces which tend to distribute the injected water over the entire cross-sectional area of a core or over the entire thickness of a bed are significant and prevent uneven saturation distribution at inlet conditions in high viscosity floods.

In the event that the subject flow system had been oil-wet a different explanation, as to the effect of rate on displacement efficiency, would have been necessary. In oil-wet systems water does not imbibe but must be forced into all flow channels. Less pressure is required to penetrate large channels, than small channels. At low rates water flows through large channels, while higher rates result in penetration of smaller channels. As a result displacement efficiency increases with rate. Displacement efficiency will increase with rate until the imposed pressure gradient is larger than the capillary pressure gradient which prevents water from entering small flow channels at low

rates. Once the capillary forces are overcome the displacement efficiency should stabilize.

Figure 10 also indicates that displacement efficiency increases with rate. In addition it discloses that displacement efficiency decreases as the volume of water injected increases for any particular flood. This decrease in displacement efficiency with increasing water injection continues until the flood front reaches the exterior boundary of the model. Once the exterior boundary is contacted the displacement efficiency begins to increase with increases in the volume of injected water. All six floods represented in Figure 10 follow this pattern.

Figures 9 and 13 indicate that areal sweep efficiency is greatly affected by the rate of injection. Both series of floods exhibited decreasing areal sweep efficiency with increasing rate up to a maximum rate, after which, further increases in rate do not affect the area swept.

As pointed out previously in the discussion on "displacement efficiency" it is believed that imbibition is the controlling factor at low rates in water-wet systems. If this fact is accepted as true, then it must be concluded that this imbibition phenomena is the reason for the very high areal sweep efficiency at low rates. The high oil recoveries (measured), also experienced at low rates, (oil recovery also decreased with increasing rate - See Figure No. 8 and No. 12) indicate that the sand pack was of a homogeneous nature, being composed of a high percentage of small uniform flow channels favorable for imbibition.

Increases in flood rates increase the "displacement efficiency" by pushing more water into larger channels, thus limiting the amount of water available for the smaller channels and providing a more uniform distribution of water throughout the bed. This occurence leads directly to a reduction in areal sweep efficiency. The large amount of subordinate production at low rates also indicates that the displacement efficiency was initially low during floods conducted at low rates.

As can be seen from Figures 9 and 13 the water flood series conducted with the higher oil-water viscosity ratio (Series 3) exhibits a greater reduction in areal sweep efficiency per unit increase in the rate of injection, than the low viscosity floods (Series 1). This point can be explained as follows. A study by P.M. Blair (See Reference 6, page 165) disclosed that imbibition is not only a function of wettability but also of the viscosity ratio of the fluids employed. Blair has shown that imbibition is more complete (ie: penetrates more of the flow channels) for low viscosity fluids than for high viscosity fluids. Therefore it can be stated that in the case of the low oil-water viscosity floods (Series 1) the majority of the flow channels are flooded at the low injection rates. Thus increases in injection rates will provide only a small increase in displacement efficiency. In the case of the high viscosity floods (Series 3) the imbibition process is not as complete due to the high oil viscosity; consequently, increases in injection rates cause a greater percentage of flow channels to be flooded resulting in a faster increase in displacement efficiency and hence a faster decline in areal sweep efficiency. The larger subordinate production in the high viscosity series (see Figure 8 at low rates) as

compared to the subordinate production in low viscosity floods (See Figure 12) also indicates that spontaneous imbibition is not as complete in the high viscosity floods as in the low viscosity floods.

Since all three efficiencies are related by the following expression:-

$$\text{Oil Recovery} = E_{as} \times E_d \times \text{P.V. of unit area} \qquad (5)$$

it is understandable that a particular behavior in one will be reflected in the others. It is obvious from the figures 11 and 14 that the imbibition phenomena or capillary forces exhibited a far greater influence on areal sweep efficiency than it did on displacement efficiency during the subject tests. As a consequence the resulting oil recovery (E_s) followed the pattern set by the behavior of the areal sweep efficiency term. That is, oil recovery decreased with increasing rate. This is contrary to results reported by Rapoport.[23] Rapoport's publication is the only known report which has investigated the effect of rate on oil recovery in two-dimensional systems. The fact that the system used by Rapoport was oil-wet is considered to be the reason that oil recovery increased with increasing injection rates rather than decrease, as was the case in the subject study.

In the water-wet system employed in this study, imbibition is considered as the reason for the very high areal sweep efficiencies and consequently the high oil recovery at low rate. Since water does not imbibe into oil-wet system but must be forced into all flow channels it is reasonable to assume that areal sweep efficiency should increase with increasing rate rather than decrease. Therefore with both areal sweep efficiency and displacement efficiency increasing with increasing injection

rate, oil recovery must follow the same pattern.

Re-examining the figures connected with this critical rate study indicates that Flood Series 3 stabilizes at approximately 12.1 B/D/ft (1680 cc/hr) which corresponds to a critical scaling coefficient of 5.4×10^{-3}. Flood Series 1 appears to stabilize between 4.05 B/D/ft (560 cc/hr) and 8.1 B/D/ft (1120 cc/hr) which corresponds to a critical scaling coefficient of 2.8×10^{-3}. It is interesting to note at this point that the above mentioned values of the critical scaling coefficient are approximately the same magnitude as those reported by Rapoport[23] (ie: between 3.5×10^{-3} and 7.4×10^{-3}).

The fact that the two critical rate are different was expected. One of the basic principles of the concept of a critical scaling coefficient is that it applies only to systems with the same viscosity ratio. Thus, if the viscosity ratio changes, the rate at which a flood stabilizes must also change.

PRODUCTION AND INJECTION HISTORY

Results

Six floods were selected for use in the final correlations. They are identified as follows:

Flood No. 1-c - Oil-water viscosity ratio of 1.68

Flood No. 2 - Oil-water viscosity ratio of 3.25

Flood No. 3-d - Oil-water viscosity ratio of 6.27

Flood No. 4 - Oil-water viscosity ratio of 8.01

Flood No. 5 - Oil-water viscosity ratio of 12.41

Flood No. 6 - Oil-water viscosity ratio of 0.5007

The production histories of the above floods are presented in Tables 7, 10, 14, 17, 18 and 19 respectively. Figures 15 and 16 present the oil recovery as a function of the viscosity ratio and volume of water injected for the various floods. Figure 15 expresses oil recovery as a percent of the original oil in place in the unit pattern. Figure 16 expresses oil recovery as a percent of the total pore volume of the unit pattern. Figures 18 to 23 inclusive show the producing water-oil ratio versus volume of oil recovered and volume of water injected. (See Appendix A).

Figures 15 and 16 disclose that oil recovery decreases with increasing oil-water viscosity ratio for any particular volume of water injected. The one exception to this pattern is Flood No. 6. The deviation of this flood will be explained later. Total recovery, after approximately 25 pore volumes of water were injected, varies from 750% to 260% of the original oil in place in the unit pattern. Since the effect of the viscosity ratio on oil recovery to water breakthrough is not discernable from Figures 15 and 16 another plot was employed. Figure 17 presents oil recovery at breakthrough versus the oil-water viscosity ratio. (Data presented in Table 34) Breakthrough recovery for both the direct offset and diagonal offset wells are represented. Both sets of wells indicate that oil recovery decreases with increasing oil-water viscosity ratio. Breakthrough recovery (at direct offsets) varies from 98.5% to 54.9% of the original oil in place over the viscosity range studied.

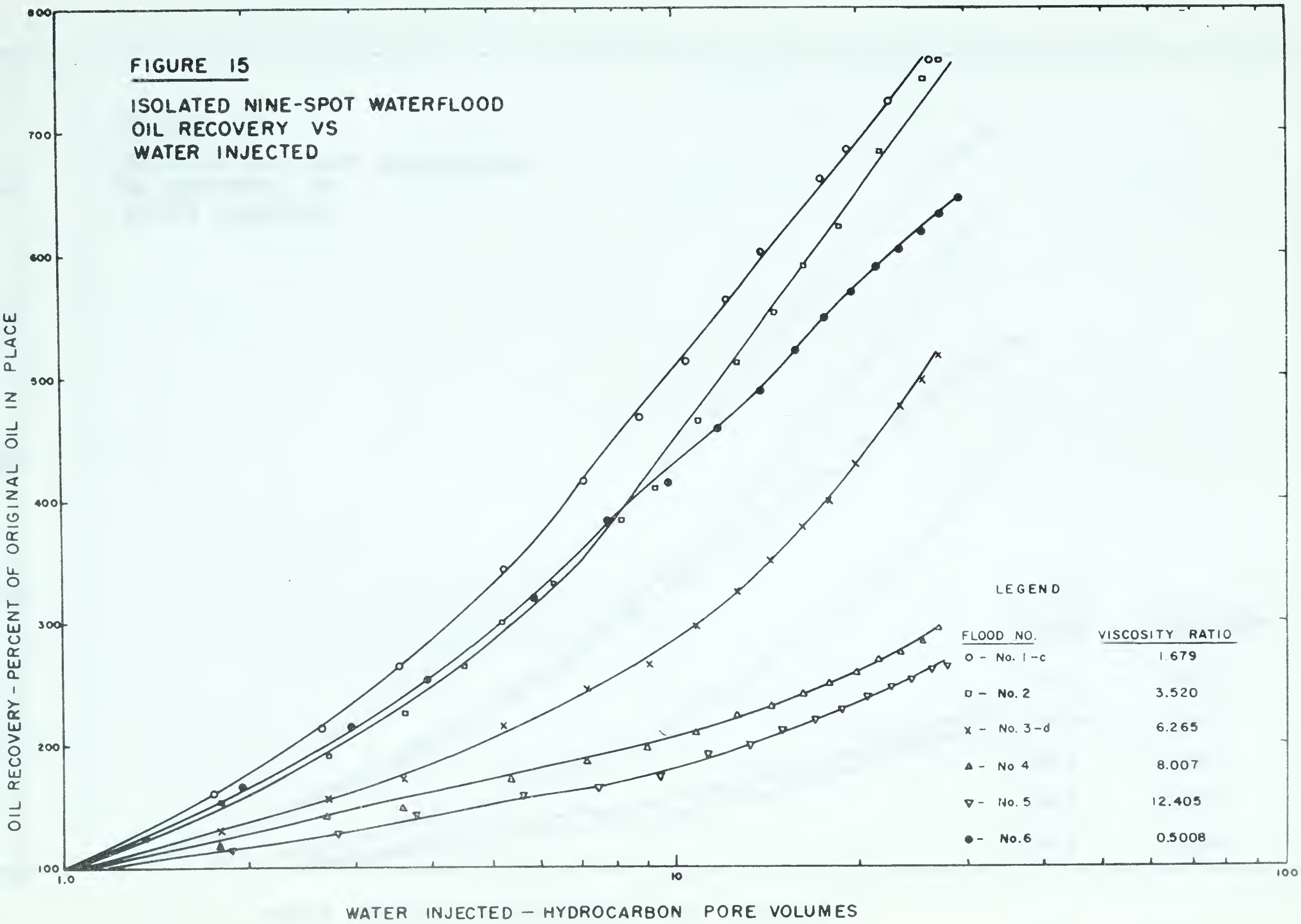
FIGURE 15
ISOLATED NINE-SPOT WATERFLOOD
OIL RECOVERY VS
WATER INJECTED
OIL RECOVERY - PERCENT OF ORIGINAL OIL IN PLACE
WATER INJECTED — HYDROCARBON PORE VOLUMES
800
700
600
500
400
300
200
100
1.0
10
100
LEGEND
FLOOD NO.
VISCOSITY RATIO
○ - No. 1-c
1.679
□ - No. 2
3.520
x - No. 3-d
6.265
▲ - No 4
8.007
▽ - No. 5
12.405
● - No. 6
0.5008

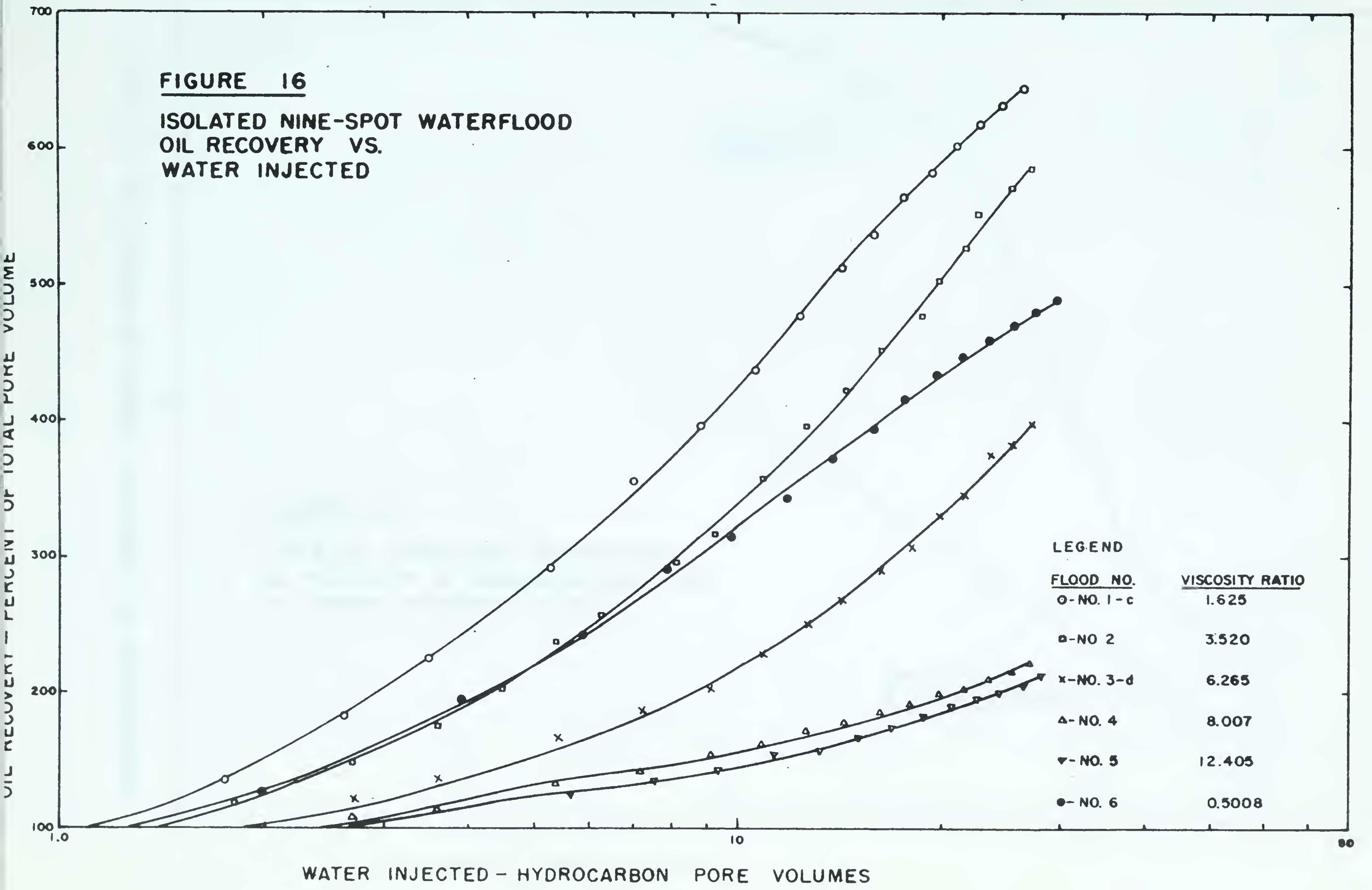

FIGURE 16

ISOLATED NINE-SPOT WATERFLOOD
OIL RECOVERY VS.
WATER INJECTED

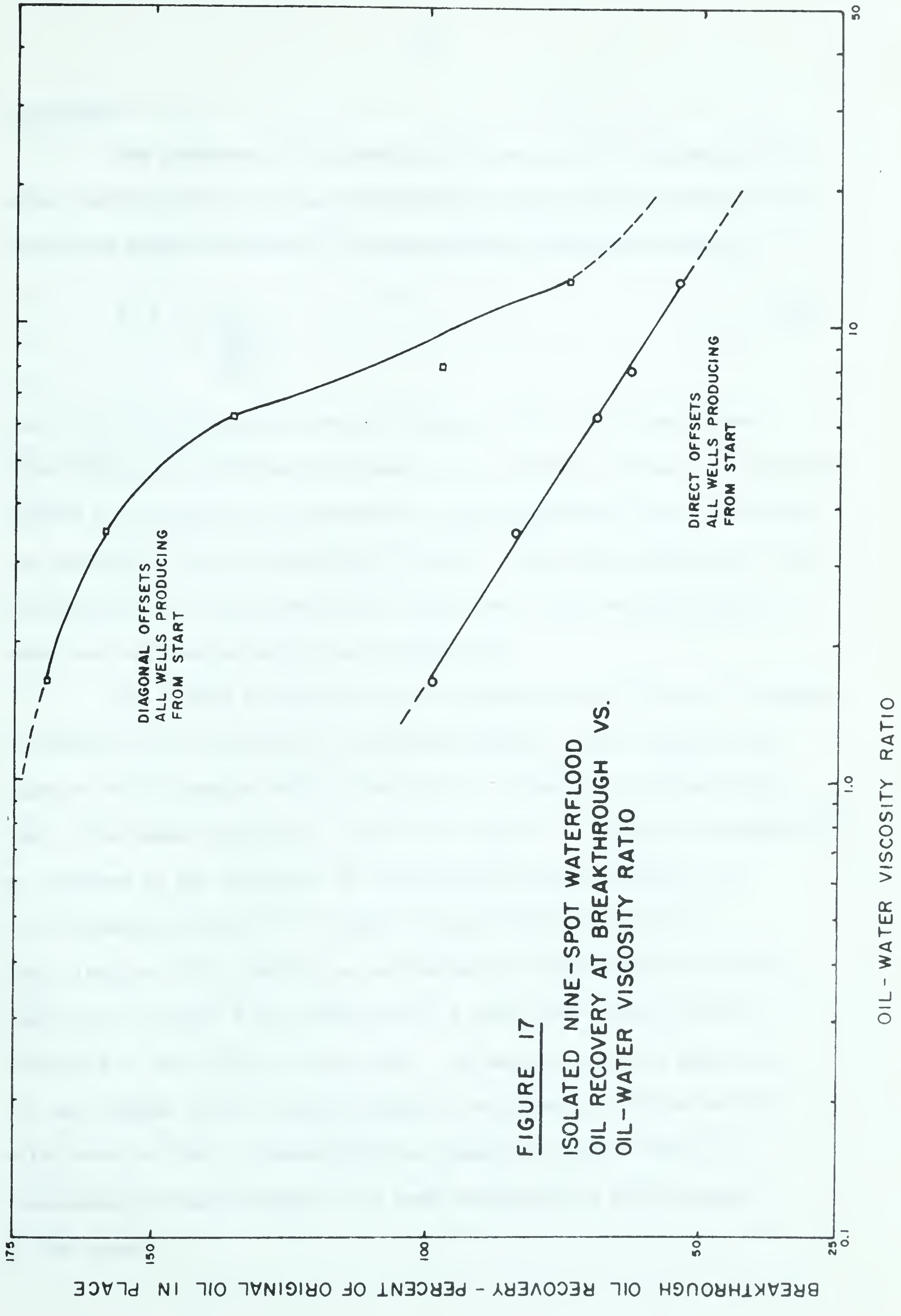

FIGURE 17

ISOLATED NINE-SPOT WATERFLOOD OIL RECOVERY AT BREAKTHROUGH VS. OIL-WATER VISCOSITY RATIO

Discussion

The phenomena of decreasing oil recovery with increasing oil-water viscosity ratio can be theoretically explained by referring to the simplified Buckley-Leverett(3) fractional-flow formula for water:

$$f_w = \frac{1}{1 + \dfrac{K_o \mu_w}{K_w \mu_o}} \tag{10}$$

where f_w is the fraction of water flowing in the total flow stream. Other terms are as defined previously. Any increase in the oil viscosity results in a reduction in magnitude of the denominator thus increasing the fraction of water flowing in a system at any given saturation of the invading fluid. This behavior has been known since the early days of petroleum engineering and is an accepted fact.

All floods followed the above pattern except Flood 6. In order to conduct this flood under a favorable mobility ratio, glycerol was added to the injection water increasing the viscosity to three times that of the water employed in the other floods. According to Rapoport(23) an increase in the viscosity of the displacing phase results in a corresponding decrease in the rate of injection necessary for stabilization. This factor was not taken into consideration and thus inadvertently Flood 6 was conducted at a rate three times the rate indicated by the critical rate study. By employing such a high rate oil was trapped in the smaller channels resulting in oil recoveries which were too low. Consequently the results of Flood 6 are unrepresentative and therefore have been excluded from the remainder of the report.

Examination of the water-oil ratio graphs (Figure 18 to 23) indicate that a scattering of data points exists. This scattering tends to become worse as the oil-water viscosity ratio increases. This behavior can be explained by the fact that as the oil-water viscosity ratio increases the flood front becomes more irregular and even slight fingering occurs. This tends to produce irregular behavior of the water-oil ratio.

AREAL SWEEP EFFICIENCY

Results

Data obtained on areal sweep efficiency as a function of mobility ratio and volume of water injected is presented in Tables 22, 24, 28, 31, 32 and 33 and Figures 24 to 27 inclusive. The tabulated data consists of measured areal sweep efficiency figures, calculation of displacement efficiency and mobility ratio.

Figure 24 illustrates areal sweep efficiency at breakthrough versus the mobility ratio. Two curves, one representing breakthrough as it occurred at the direct offset wells and the other representing breakthrough at the diagonal offset wells, are shown. Figure 25 shows areal sweep efficiency as a function of mobility ratio and the number of pore volumes of water injected. This plot has been patterned after the work of Dyes.[9]

Figures 26 and 27 present areal sweep efficiency as a function of total volume injected as compared to the volume injected to breakthrough, (Q/Q_{BT}) with the viscosity ratio being the parameter. The breakthrough volume in Figure 26 is the volume of fluid injected before

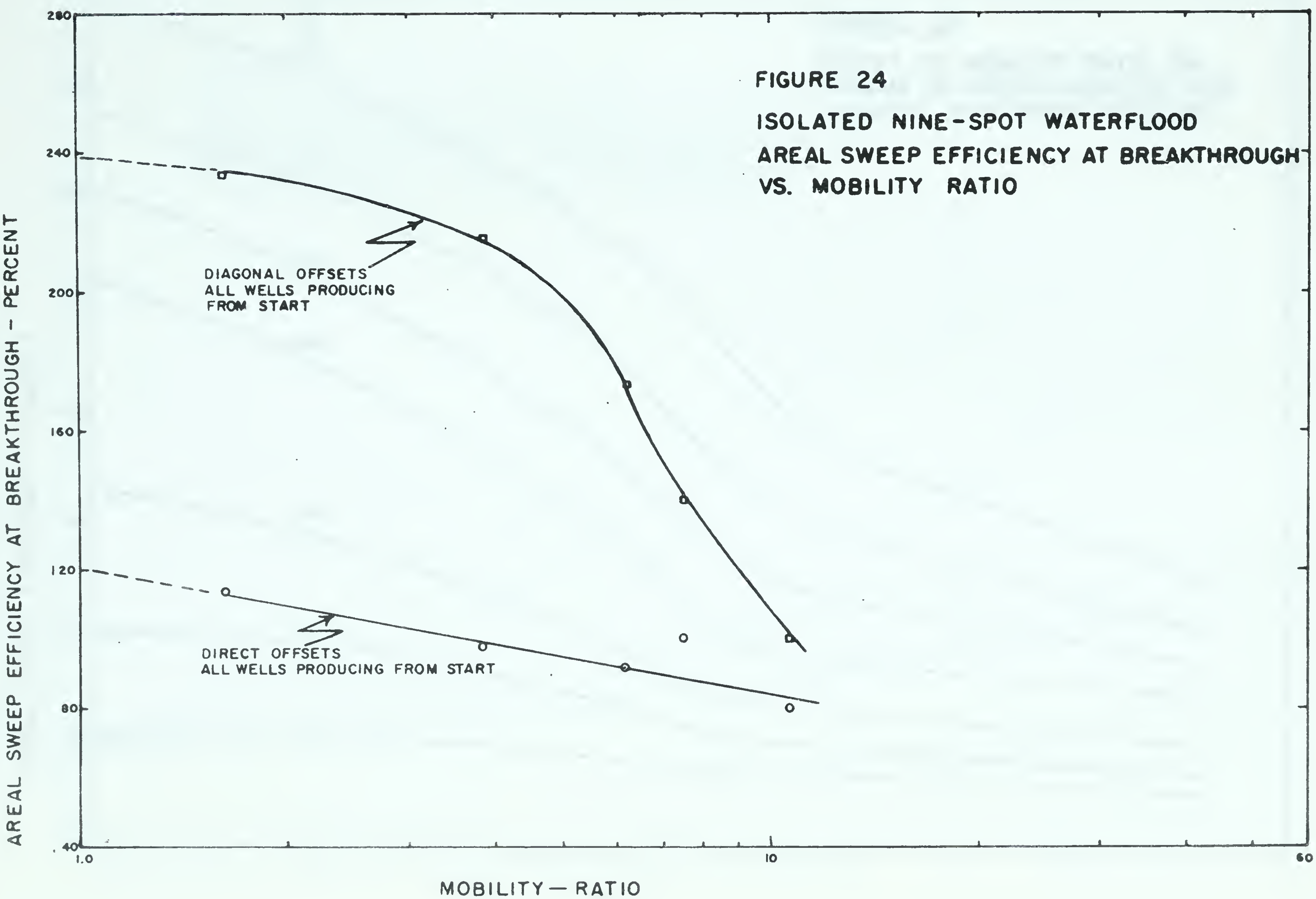

FIGURE 24
ISOLATED NINE-SPOT WATERFLOOD
AREAL SWEEP EFFICIENCY AT BREAKTHROUGH
VS. MOBILITY RATIO
DIAGONAL OFFSETS
ALL WELLS PRODUCING
FROM START
DIRECT OFFSETS
ALL WELLS PRODUCING FROM START
AREAL SWEEP EFFICIENCY AT BREAKTHROUGH - PERCENT
MOBILITY — RATIO
280
240
200
160
120
80
40
1.0
10
60

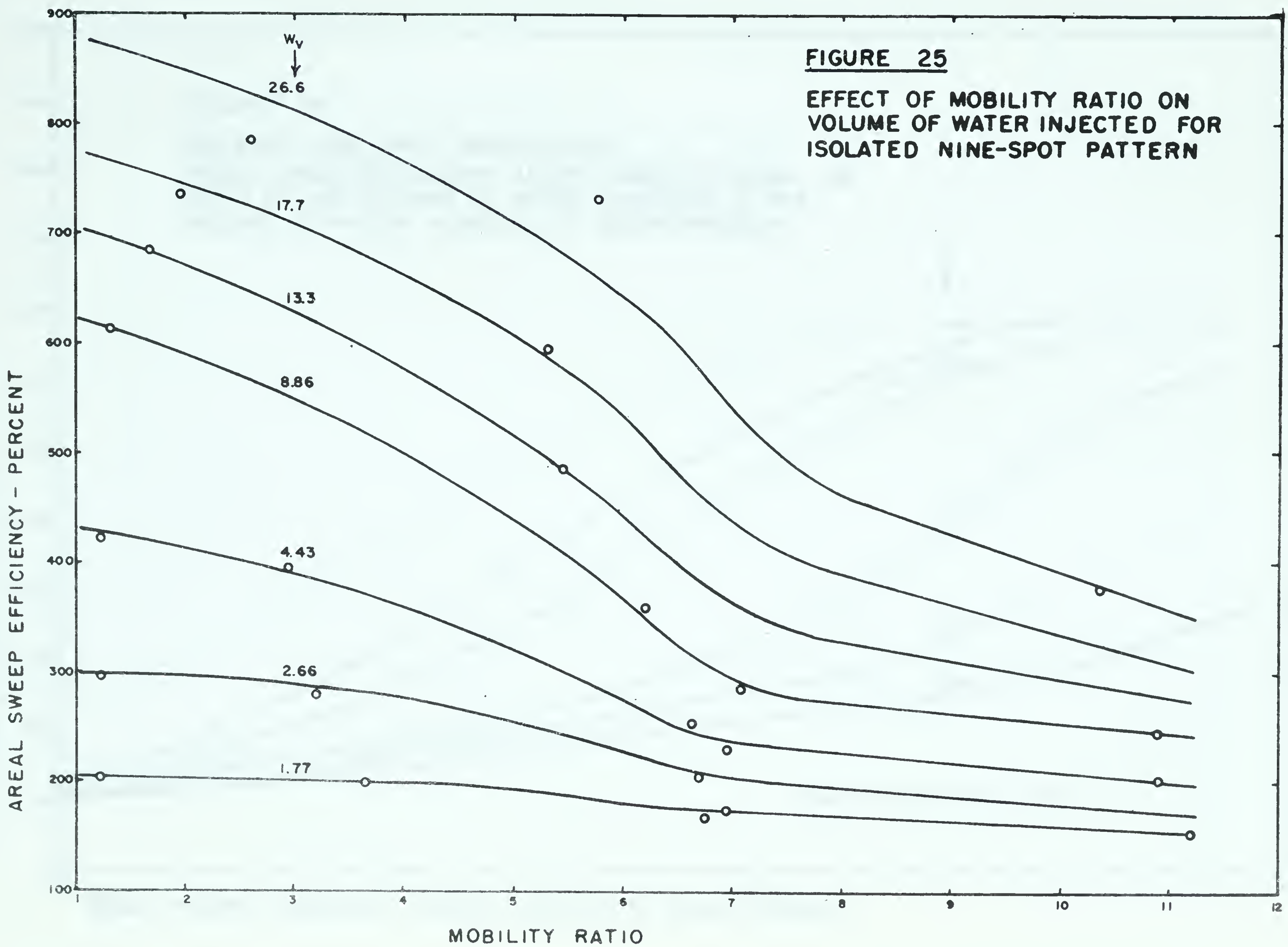

FIGURE 25

EFFECT OF MOBILITY RATIO ON VOLUME OF WATER INJECTED FOR ISOLATED NINE-SPOT PATTERN

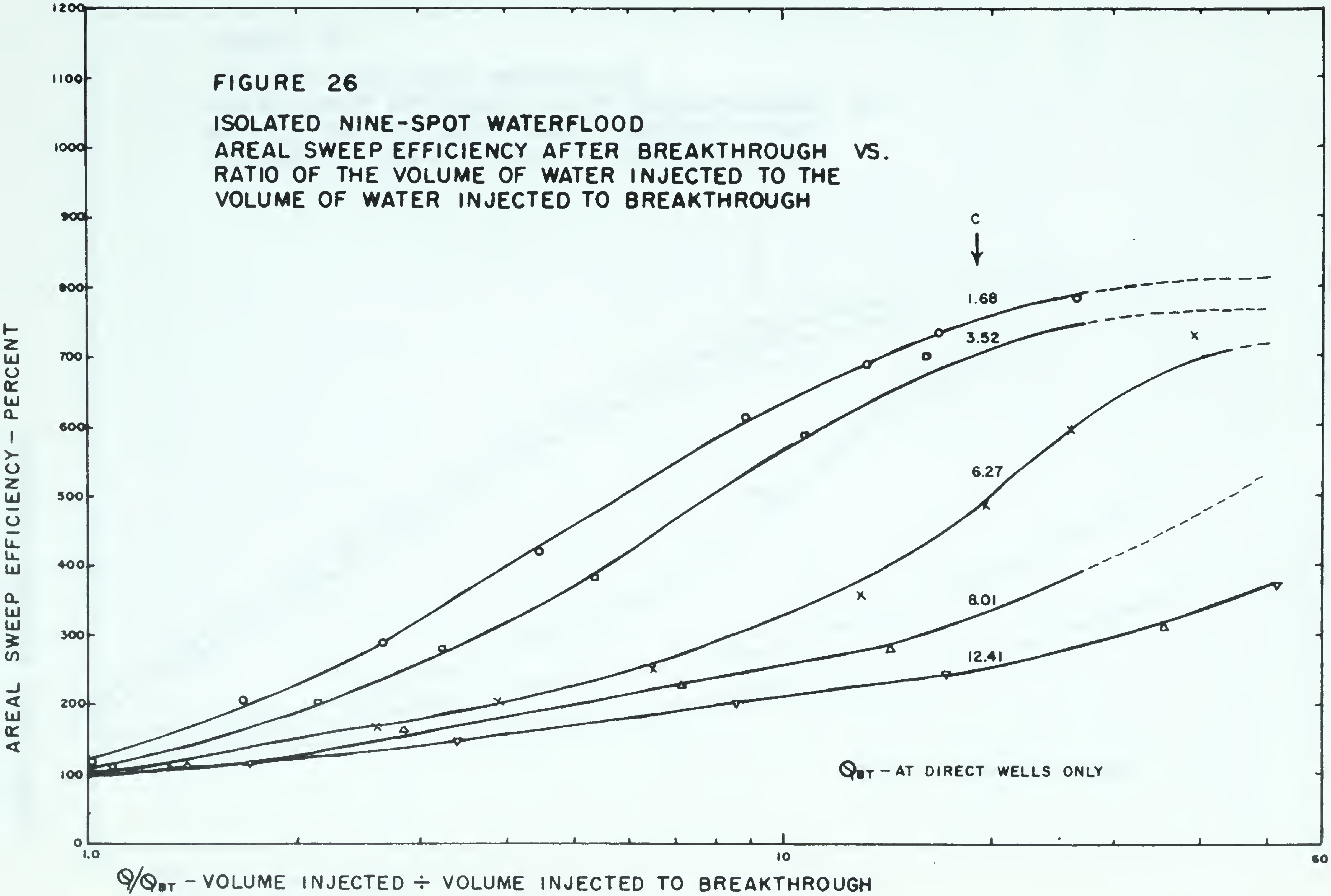

FIGURE 26

ISOLATED NINE-SPOT WATERFLOOD
AREAL SWEEP EFFICIENCY AFTER BREAKTHROUGH VS.
RATIO OF THE VOLUME OF WATER INJECTED TO THE
VOLUME OF WATER INJECTED TO BREAKTHROUGH

FIGURE 27

ISOLATED NINE-SPOT WATERFLOOD
AREAL SWEEP EFFICIENCY AFTER BREAKTHROUGH VS.
RATIO OF THE VOLUME OF WATER INJECTED TO THE
VOLUME OF WATER INJECTED TO BREAKTHROUGH

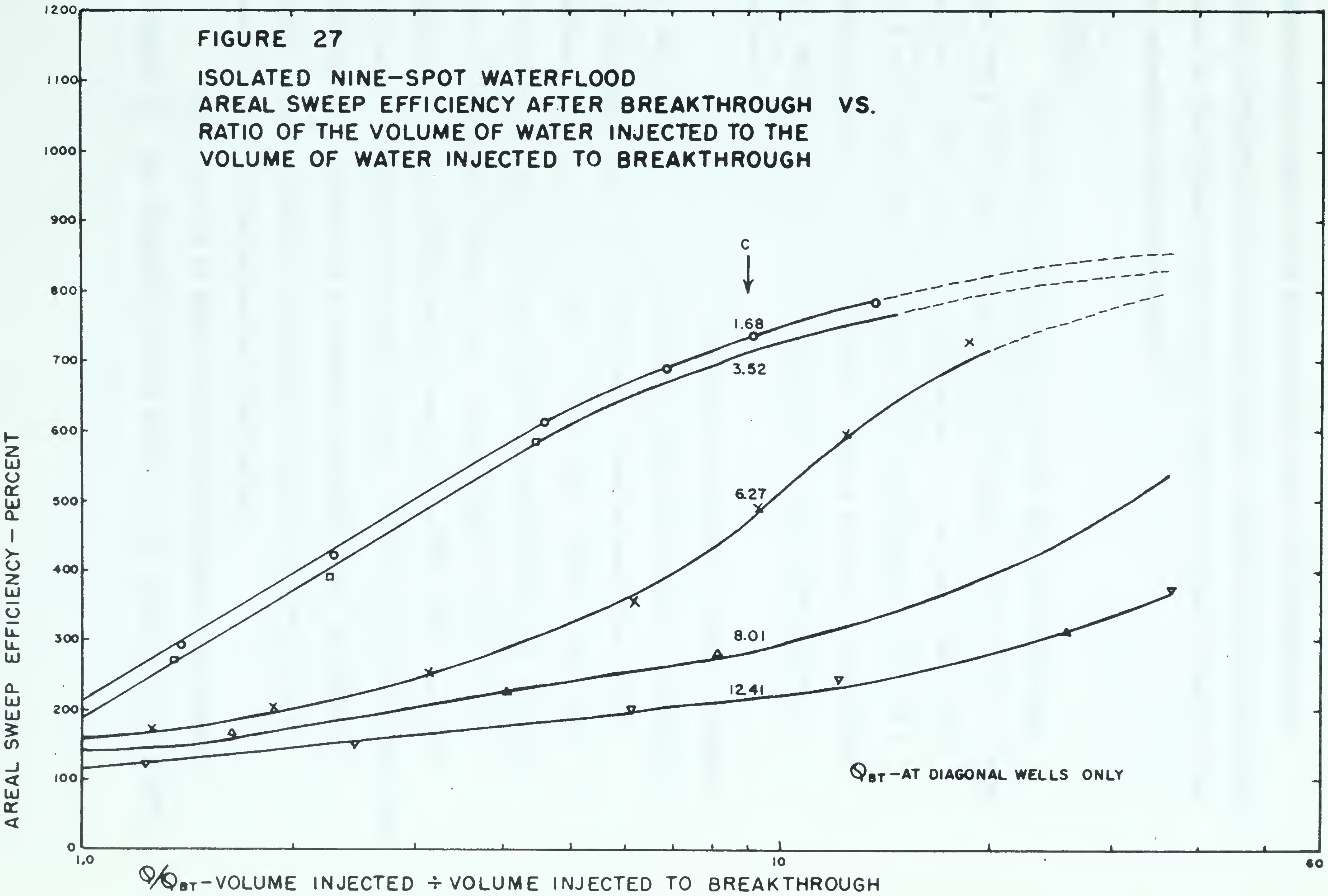

breakthrough occurs at the direct offset wells. The breakthrough volume in Figure 27 is the volume of fluid injected before breakthrough occurs at the diagonal offset wells. This type of plot is adapted from the procedure outlined by Craig.[7]

Discussion

Referring to Figure 24, it is seen that the breakthrough areal sweep efficiency increases with decreasing mobility ratio. Since mobility is often referred to as a measure of the ease with which a fluid will flow through the rock, it is understandable then that a larger area will be contacted by the injected fluid as the mobility ratio decreases. This type of behavior has been substantiated by numerous other authors.

Due to the lack of published literature on isolated systems it was very difficult to obtain data for comparison purposes. According to a confidential data source there are no results available for an isolated nine-spot such as used in this study. However, data was obtained on a confined nine-spot pattern (confidential data source). The areal sweep efficiency at water breakthrough for unit mobility, considering the direct offset wells, was given as 80%. This compares to a value of 120% from the subject system. However, since the comparison is between an isolated and a confined system and since the method of analysis used to evaluate the confined pattern is unknown, it is doubtful if the collation has any significance.

The same type of behavior as noted in Figure 24 is repeated in Figure 25. The parameter in this figure is the number of pore volumes

of injected water. Although high ultimate sweep out patterns are obtained for most mobility ratios, Figure 25 illustrates that considerably more area is swept at lower mobilities than at high mobilities for the same volume of water injected. Thus, from an economic standpoint the rate of oil recovery and the total amount of fluid to be injected cause the lower mobility floods to be much more favorable.

Figures 26 and 27 are essentially the same as Figure 25. The only difference is that the volume injected is expressed as Q/Q_{BT} and is plotted as the ordinate instead of being utilized as a parameter. The mobility ratio varies during a flood hence it could not be used as a parameter and therefore the viscosity ratio was introduced. As pointed out previously the difference between Figures 26 and 27 is in the definition of the volume injected to breakthrough. Both graphs yield identical results and thus either one can be used. This is clearly illustrated by the following example.

Assuming that the oil-water viscosity ratio of a hypothetical reservoir is approximately 3.52 and that the volume injected before breakthrough at the direct wells is 61.6 and at the diagonal wells is 128.5. The areal sweep efficiency at $Q/Q_{BT} = 10.0$ is 330% from Figure 27. The total volume injected up to this time is 10 x 61.6 or 616. Thus the equivalent Q/Q_{BT} for the diagonal offset plot is $616 \div 128.5$ or $Q/Q_{BT} = 4.8$. The areal sweep efficiency at $Q/Q_{BT} = 4.8$ for a 3.5 oil-water viscosity ratio (from Figures 27) is 320%. Thus, both figures yield approximately the same results.

Further examination of either Figure 26 or 27 discloses that the top three curves in both figures appear to be levelling off or

reaching a maximum. This levelling off can be attributed to a boundary effect. Up until this point the bed has acted essentially as an infinite reservoir. It is noticed that these three curves tend to level off at the same value of areal sweep efficiency ie: 650%. Reconverting this into areal coverage yields an area, which if considered as a circle, has a diameter approximately equal to the dimension of the model. The bottom two curves (ie: high viscosity floods) have not yet shown signs of levelling off. This is due to the fact that the areal coverage of the injected fluid has not as yet extended to the outer edge of the model.

PRACTICAL APPLICATION

In determining the economic worthiness of a secondary recovery project, the area of the reservoir which will be swept by the invading fluid is of great importance. Most literature pertaining to sweep efficiency has emphasized the pattern which is obtained at breakthrough of the invading fluid. However, the increase in areal sweep efficiency which occurs after breakthrough has been demonstrated to be of significant proportions.[7,9,17] This is particularly true in the case of an isolated system, as is demonstrated by the subject report. Thus, to accurately determine the economics of a system, one must know the sweep efficiency at breakthrough and also the continual enlargement of the pattern which occurs during production after breakthrough.

The data presented in the subject report can be applied to water flood calculations by using the technique proposed by Craig.[7]

This procedure utilizes Welge's[25] method in conjunction with laboratory data obtained on areal sweep efficiency after breakthrough for a five-spot pattern. By using Figures 24 and 26, to determine the manner in which the areal sweep efficiency changes with continued water injection, the calculations can be revised for an isolated nine-spot pattern.

It is also important to realize that the data obtained from the model used in this study represents a steady state injection operation in an entirely liquid filled reservoir. (ie: no free gas, above bubble point). In addition the model represents a reservoir of constant thickness with impermeable barriers above and below the producing zone. The porous media being represented by a unconsolidated sand pack with uniform permeability and porosity. The data presented only illustrates the effect of mobility ratio and volume of water injected on areal sweep efficiency. All other factors are constant.

CONCLUSIONS

Treatment of water flood behavior in two-dimensional systems as encountered in the reservoir can best be studied by scaled flow model experiments. In the displacement of oil by water in these two-dimensional flow systems capillary forces are of paramount importance. In all cases, results obtained by this approach must be attained under conditions in which the water-oil displacement is no longer influenced by capillary effects.

The results of this study led to the following conclusions:

1. The most important factor in scaling an oil field reservoir was found to be the capillary effects. This study has shown that for sufficiently high injection rates the flooding behavior can be expected to be rate independent or stabilized. Only under stabilized conditions can laboratory results be utilized for field evaluations.

2. The study of the effect of injection rate on the performance of a water-wet two-dimensional system has shown that oil recovery decreases with increasing rate until stabilized conditions are obtained.

3. Area much in excess of the unit pattern is swept by the invading fluid when production is continued to high water-oil ratios.

4. Oil recoveries far exceeding the amount of oil originally in place in the unit pattern is produced when production is continued to high water-oil ratios.

5. Lower oil recoveries and smaller areal coverage occurs when more viscous oils (ie: higher mobility ratio) are used as the displaced phase.

6. High ultimate sweep out patterns were obtained for all mobility ratios studied. However, considerably more area is swept at lower mobilities than at high mobilities for the same volume of water injected. Therefore from an economic standpoint the lower mobility floods are much more favourable.

7. This study has shown that isolated floods are very much different than confined water floods. Therefore it is essential that when a water flood development is under study recognition of the difference between the two patterns is imperative.

8. At high water-oil ratios, sufficient reservoir has been swept so that the isolated model pattern no longer acts as if it were an infinite reservoir and boundary effects influence the performance.

REFERENCES CITED

1. Adam, N.K., "The Physics and Chemistry of Surfaces", Oxford University Press, 3rd Edition (1941).

2. Bobek, J.E., Mattax, C.C., Denekas, M.O., "Reservoir Rock Wettability - Its Significance and Evaluation", A.I.M.E. Trans. Vol. 213 (1958).

3. Buckley, S.E., Leverett, M.C., "Mechanism of Fluid Displacement in Sands", A.I.M.E. Trans. Vol. 146 (1942).

4. Caudle, B.H., Erickson, R.A., Slobod, R.L., "The Encroachment of Injected Fluids Beyond the Normal Well Pattern", A.I.M.E. Trans. Vol. 204 (1955).

5. Caudle, B.H., Loncaric, I.G., "Oil Recovery in Five-Spot Pilot Floods", Corpus Christi A.I.M.E. Meeting (1959).

6. Collins, R.E., "Flow of Fluids Through Porous Materials", Reinhold Publishing Corporation, New York (1961).

7. Craig, F.F., Geffen, T.M., Morse, R.A., "Oil Recovery of Pattern Gas or Water Injection Operations for Model Tests", A.I.M.E. Trans. Vol. 204 (1955).

8. Dalton, R.L., Rapoport, R.A., Carpenter, C.W., "Laboratory Studies of Pilot Water Floods", A.I.M.E. Trans. Vol. 219 (1960).

9. Dyes, A.B., C audle, B.H., Erickson, R.A., "Oil Production After Breakthrough as Influenced by Mobility Ratio", A.I.M.E. Trans. Vol. 219, (1954).

10. Engelberts, W.F., Klinkenberg, L.F., "Laboratory Experiments on the Displacement of Oil by Water from Packs of Granular Material", The Third World Petroleum Congress (1951).

11. Jones-Parra, J., Stahl, C.D., Calhoun, J.C., "A Theoretical and Experimental Study of Constant Rate Displacements in Water-Wet Systems", Producers Monthly, Vol. 18 (1953-54).

12. Kyte, J.R., Rapoport, R.A., "Linear Waterflood Behavior and End Effects in Water-Wet Porous Media", A.I.M.E. Trans. Vol. 213 (1958).

13. Lee, B.D., "Potentiometric-model Studies of Fluid Flow in Petroleum Reservoirs", A.I.M.E. Trans. Vol. 174 (1948).

14. Leverett, M.C., "Capillary Behavior in Porous Media", A.I.M.E. Trans. (1941).

15. Maguss, H., "Waterflood Behavior in Linear Systems", unpublished manuscript, M.Sc. Thesis, University of Alberta, (1962).

16. Muskat, M., "Physical Principles of Oil Production", McGraw Hill Book Company, Inc. (1949).

17. Neilson, I.D.R., "The Effect of a Free Gas Saturation on the Sweep Efficiency of an Isolated Inverted Five-Spot", unpublished manuscript, M.Sc. Thesis, University of Alberta, (1960).

18. Newcombe, J., McGhee, J., Rzasa, M.J., "Wettability versus Displacement in Waterflooding Unconsolidated Sand Columns", A.I.M.E. Trans. Vol. 204 (1955).

19. Pirson, S.J., "Oil Reservoir Engineering", McGraw Hill Book Company, Inc., (1958).

20. Pritchard, K.C.G., "A Model Study of an Unconsolidated Sandstone System", unpublished manuscript, M.Sc. Thesis, University of Alberta, (1962).

21. Rapoport, L.A., Leas, W.J., "Properties of Linear Waterfloods", A.I.M.E. Trans. Vol. 198 (1953).

22. Rapoport, L.A., "Scaling Laws for Use in Design and Operation of Water-Oil Flow Models", A.I.M.E. Trans. Vol. 204 (1955).

23. Rapoport, L.A., Carpenter, C.W., Leas, W.J., "Laboratory Studies of Five-Spot Waterflood Performance", A.I.M.E. Trans. Vol. 213 (1958).

24. Slobod, R.L., Caudle, B.H., "X-ray Shadowgraph Studies of Areal Sweepout Efficiencies", A.I.M.E. Trans. Vol. 195 (1952).

25. Welge, H.J., "A Simplified Method for Computing Oil Recovery by Gas or Water Drive", A.I.M.E. Trans. Vol. 195 (1952).

26. Weyl, W.A., Sonders, L.R., and Enright, D.P., "Wettability, a Function of the Polarizability of the Surface Ions", Journal of Applied Physics, Vol. 21 (1950).

27. Wykoff, Botset and Muskat, "The Mechanics of Porous Flow Applied to Waterflooding Problems", A.I.M.E. Trans. Vol. 103 (1933).

APPENDIX A

Table 1

CALCULATION OF ABSOLUTE PERMEABILITY

Muskat's Equation:

$$Q = \frac{0.003541 \, \Delta P \, K \, h}{\mu_w \, \beta \left[\log d/r_w - 0.619\right]}$$

For five-spot pattern.

where:

Q - injection rate in B/D

ΔP - pressure differential in psi

K - permeability in millidarcys

h - formation thickness in feet

μ_w - water viscosity in centipoises

β - formation - volume factor (1)

d - distance from injection well to producing well in feet

r_w - well bore radius in feet

Model and Fluid Characteristics:

$Q = 0.278$ B/D

$\Delta P = 0.320$ psi

$h = 0.0208$ ft

$\mu_w = 0.8837$ cp

$\beta = 1.0$

$\log d/r_w = 4.92$

$$K = \frac{0.278 \times 1.0 \times 0.8837 \times (4.92 - .619)}{0.003541 \times 0.320 \times 0.0208}$$

$K = 43{,}500$ md

Compares favorably with Pritchard's[20] permeability of 40,700 md.

Table 2

GEOMETRIC AND RESERVOIR PROPERTIES OF THE MODEL

Length	32 inches
Width	32 inches
Thickness	1/4 inch
Length (Unit Area)	8 inches
Porosity	Pack I - 44.07%
	Pack II - 40.75%
Total Pore Volume of Unit Area	Pack I - 115.55 cc
	Pack II - 106.85 cc
Scaling Coefficient "C_2" *	Pack I - q x 4.58×10^{-4}
	Pack II - q x 4.42×10^{-4}

$$^{*}\ C_2 = \frac{q\,\mu_w}{\sigma_{ow}\cos\theta\sqrt{K\,\phi}}$$

where C_2 is employed on graphs

q	- B/D/ft
μ_w	- cp
σ_{ow}	- dyne/cm
K	- md
ϕ	- fraction
θ	- taken as 60°

Table 3

FLUID PROPERTIES

Flood No.	Viscosity Oil	Viscosity Water	Density Oil	Density Water	Interfacial Tension
1	1.595	0.95	0.8098	1.000	32.14
2	3.342	0.95	0.8311	1.000	32.04
3	5.592	0.95	0.8463	1.000	31.34
4	7.607	0.95	0.8209	1.000	29.63
5	11.786	0.95	0.8469	1.000	32.04
6	1.595	3.185	0.8098	1.094	30.17

Viscosity is in centipoises

Density is in grams/cc

Interfacial tension is in dynes/cm

Table 4

Production History - Nine-Spot Flood I

Injection Rate = 320 cc/hr S_{cw} = 20.70% μ_o = 1.595

(1) Total Cum. Production	(2) Cum. Wtr. Production	(3) Cum. Oil Production	(4) Inst. W.O.R.	(5) Oil Rec. in Hydro. P.V.	(6) Water Inj. in Hydro. P.V.
80	1	79	0.00125	0.945	0.945
160	17	143	0.250	1.670	1.895
240	30	210	0.194		
320	46	274	0.250	3.24	3.78
400	66	334	0.333		
480	91	389	0.455	4.60	5.67
560	123	437	0.667		
640	156	484	0.703	5.72	7.57
720	214	506	2.640		
800	271	529	2.480	6.25	9.45
880	334	546	3.700		
960	402	558	5.650	6.60	11.35
1040	473	567	7.890		
1120	545	575	9.000	6.80	13.25
1200	618	582	10.400		
1280	692	588	12.320	6.95	15.18
1360	767	593	15.000		
1440	843	597	19.000	7.06	17.00
1520	919	601	19.000		
1600	995	605	19.000	7.15	18.92
1680	1072	608	25.650		
1760	1147	613	15.000	7.25	20.08
1840	1222	618	15.000		
1920	1301	619	79.000	7.26	22.70
2000	1378	622	25.650		
2080	1455	625	25.650	7.40	24.60
2160	1532	628	25.650		
2240	1610	630	39.000	7.44	26.50
2320	1689	631	79.000		
2400	1768	632	79.000	7.48	28.40

Table 5

Production History - Nine-Spot Flood I-a

Injection Rate = 560 cc/hr S_{cw} = 19.69% μ_o = 1.595 cp

(1) Total Cum. Production	(2) Cum. Str. Production	(3) Cum. Oil Production	(4) Inst. W.O.R.	(5) Oil Rec. in Hydro. P.V.	(6) Water Inj. in Hydro. P.V.
80	--	80	0.000	0.932	0.932
160	25	135	0.455	1.575	1.870
240	48	192	0.404		
320	79	241	0.632	2.81	3.72
400	111	289	0.667		
480	145	335	0.738	3.90	5.60
560	184	376	0.952		
640	232	408	1.500	4.76	7.46
720	283	437	1.760		
800	338	462	2.200	5.37	9.32
880	398	482	3.000		
960	461	499	3.710	5.82	11.20
1040	528	512	5.150		
1120	593	527	4.330	6.15	13.05
1200	665	535	9.000		
1280	736	544	7.890	6.33	14.95
1360	808	552	9.000		
1440	881	559	10.400	6.52	16.75
1520	955	565	12.320		
1600	1030	570	15.000	6.65	18.70
1680	1105	575	15.000		
1760	1181	579	19.000	6.75	20.50
1840	1257	583	19.000		
1920	1332	588	15.00	6.85	22.40
2000	1409	591	25.650		
2080	1485	595	19.00	6.93	24.22
2160	1561	599	19.00		
2240	1639	601	39.00	7.00	26.10
2320	1717	603	39.00		
2400	1795	605	39.00	7.05	28.00

Table 6

Production History - Nine-Spot Flood I-b

Injection Rate = 1120 cc/hr S_{cw} = 17.25% μ_o = 1.595 cp

(1) Total Cum. Production	(2) Cum. Wtr. Production	(3) Cum. Oil Production	(4) Inst. W.O.R.	(5) Oil Rec. in Hydro. P.V.	(6) Water Inj. in Hydro. P.V.
80	--	80	0.000	0.9025	0.9025
160	18	142	0.291	1.600	1.809
240	43	197	0.455		
320	79	241	0.819	2.72	3.61
400	123	277	1.221		
480	162	318	0.952	3.59	5.42
560	206	354	1.221		
640	257	383	1.760	4.32	7.22
720	310	410	1.965		
800	367	433	2.480	4.89	9.03
880	424	456	2.480		
960	483	477	2.810	5.375	10.83
1040	546	494	3.700		
1120	608	512	3.440	5.78	12.65
1200	674	526	4.570		
1280	739	541	4.330	6.11	14.50
1360	807	553	5.660		
1440	878	562	7.890	6.34	16.25
1520	948	572	7.000		
1600	1018	582	7.000	6.57	18.09
1680	1089	591	7.890		
1760	1164	596	15.000	6.73	19.89
1840	1238	602	12.320		
1920	1311	609	10.400	6.86	21.70
2000	1385	615	12.320		
2080	1460	620	15.000	7.00	23.56
2160	1535	625	15.000		
2240	1610	630	15.000	7.11	25.25
2320	1687	633	25.650		
2400	1761	639	12.320	7.21	27.10

Table 7

Production History - Nine-Spot Flood I-c

Injection Rate = 1680 cc/hr S_{cw} = 15.07% μ_o = 1.595 cp

(1) Total Cum. Production	(2) Cum. Wtr. Production	(3) Cum. Oil Production	(4) Inst. W.O.R.	(5) Oil Rec. in Hydro. P.V.	(6) Water Inj. in Hydro. P.V.
80	--	80	0.000	0.879	0.879
160	14	146	0.212	1.605	1.760
240	44	196	0.600		
320	78	242	0.740	2.66	3.51
400	123	277	1.285		
480	167	313	1.220	3.44	5.27
560	213	347	1.352		
640	261	379	1.500	4.16	7.04
720	317	403	2.330		
800	375	425	2.630	4.67	8.79
880	432	448	2.480		
960	484	476	1.855	5.13	10.55
1040	545	495	3.210		
1120	609	511	4.000	5.62	12.30
1200	670	530	3.210		
1280	733	547	3.710	6.00	14.10
1360	799	561	4.000		
1440	867	573	5.650	6.30	15.80
1520	935	585	5.650		
1600	1001	599	4.700	6.59	17.60
1680	1068	612	5.150		
1760	1138	622	7.000	6.84	19.35
1840	1210	630	9.000		
1920	1278	642	5.650	7.05	21.10
2000	1350	650	9.000		
2000	1421	659	7.900	7.24	22.85
2160	1493	667	9.000		
2240	1566	674	10.400	7.40	24.60
2320	1642	678	19.000		
2400	1712	688	7.000	7.56	26.40

Table 8

Production History - Nine-Spot Flood I-d

Injection Rate = 2240 cc/hr S_{cw} = 18.82% μ_o = 1.595 cp

(1) Total Cum. Production	(2) Cum. Wtr. Production	(3) Cum. Oil Production	(4) Inst. W.O.R.	(5) Oil Rec. in Hydro. P.V.	(6) Water Inj. in Hydro. P.V.
80	0	80	0.000	0.921	0.921
160	30	130	0.600	1.500	1.845
240	74	166	1.221		
320	118	202	1.221	2.32	3.68
400	167	233	1.581		
480	210	270	1.162	3.11	5.52
560	263	297	1.965		
640	319	321	2.334	3.70	7.37
720	377	343	2.636		
800	436	364	2.810	4.19	9.21
880	494	386	2.636		
960	554	406	3.000	4.68	11.05
1040	617	423	3.700		
1120	683	437	4.714	5.03	12.80
1200	747	453	4.000		
1280	812	468	4.333	5.38	14.80
1360	880	480	5.660		
1440	946	494	4.714	5.69	16.55
1520	1018	502	9.000		
1600	1087	513	6.272	5.91	18.95
1680	1155	525	5.660		
1760	1228	532	10.400	6.13	20.30
1840	1301	539	10.400		
1920	1373	547	9.000	6.30	22.10
2000	1446	554	10.400		
2080	1519	561	10.400	6.45	23.95
2160	1590	570	7.89		
2240	1660	574	19.000	6.61	25.80
2320	1742	578	19.000		
2400	1816	584	12.32	6.72	27.70

Table 9

Production History - Nine-Spot Flood 1-e

Injection Rate = 2800 cc/hr S_{cw} = 20.25% μ_o = 1.595 cp

(1) Total Cum. Production	(2) Cum. Wtr. Production	(3) Cum. Oil Production	(5) Oil Rec. in Hydro. P.V.	(6) Water Inj. in Hydro. P.V.
80	--	80	0.939	0.939
160	34	126	1.480	1.880
320	123	197	2.318	3.75
400	190	210		
480	239	241	2.83	5.63
640	355	285	3.34	7.52
800	478	322	3.78	9.39
880	535	345		
1120	726	394	4.63	13.15
1200	790	410		
1280	857	423	4.96	15.00
1440	997	443	5.20	16.90
1600	1138	462	5.42	18.80
1680	1208	472		
1840	1352	488	5.74	21.60
2000	1498	502		
2080	1572	508	5.97	24.45
2240	1721	519	6.09	26.30
2400	1872	528	6.20	28.20

Table 10

Production History - Nine-Spot Flood 2

Injection Rate = 1120 cc/hr S_{cw} = 23.5 % μ_o = 3.342 cp

(1) Total Cum. Production	(2) Cum. Wtr. Production	(3) Cum. Oil Production	(4) Inst. W.O.R.	(5) Oil Rec. in Hydro. P.V.	(6) Water Inj. in Hydro. P.V.
80	tr.	80	0.000	0.904	0.904
160	23	137	0.222	1.55	1.804
240	70	170	0.510		
320	118	202	1.500	2.28	3.61
400	166	234	1.500		
480	210	270	1.220	3.04	5.41
560	264	296	2.08		
640	322	318	2.64	3.59	7.23
720	378	342	2.33		
800	437	363	2.81	4.10	9.25
880	491	389	2.08		
960	547	413	2.33	4.67	10.80
1040	609	431	3.45		
1120	666	454	3.71	5.12	12.65
1200	734	466	5.66		
1280	791	489	2.48	5.52	14.45
1360	853	507	3.45		
1440	917	523	4.00	5.90	16.25
1520	983	537	4.71		
1600	1047	553	4.00	6.24	18.65
1680	1111	569	4.00		
1760	1175	585	4.00	6.60	19.85
1840	1242	598	5.15		
1920	1310	610	5.66	6.88	21.65
2000	1376	624	4.71		
2080	1443	637	5.15	7.19	22.60
2160	1510	650	5.15		
2240	1579	661	6.27	7.46	25.25
2320	1655	665	19.00		
2400	1725	675	7.00	7.62	27.10

Table 11

Production History - Nine-Spot Flood 3-a

Injection Rate = 1120 cc/hr S_{cw} = 23.5% μ_o = 5.592 cp

(1) Total Cum. Production	(2) Cum. Wtr. Production	(3) Cum. Oil Production	(4) Inst. W.O.R.	(5) Oil Rec. in Hydro. P.V.	(6) Water Inj. in Hydro. P.V.
80	1	79	0.0127	0.892	0.904
160	40	120	0.95	1.350	1.805
240	93	147	1.96		
320	149	171	2.33	1.93	3.61
400	209	191	3.00		
480	264	216	2.20	2.44	5.42
560	330	230	4.71		
640	392	248	3.45	2.80	7.22
720	456	264	4.00		
800	522	278	4.71	3.14	9.04
880	579	301	2.48		
960	643	317	4.00	3.58	10.80
1040	708	332	4.34		
1120	773	347	4.34	3.92	12.65
1200	839	361	4.71		
1280	898	382	2.81	4.31	14.45
1360	961	399	3.70		
1440	1030	410	6.25	4.63	16.25
1520	1095	425	4.34		
1600	1163	436	7.90	4.92	18.05
1680	1226	454	3.45		
1760	1291	469	4.34	5.30	19.85
1840	1358	482	5.15		
1920	1429	491	7.90	5.54	21.70
2000	1497	503	5.76		
2080	1565	515	5.76	5.82	23.50
2160	1629	531	4.00		
2240	1697	541	7.00	6.10	25.30
2320	1770	550	7.90		
2400	1839	561	6.25	6.32	27.70

Table 12

Production History - Nine-Spot Flood 3-b

Injection Rate = 560 cc/hr S_{cw} = 23.5% μ_o = 5.592cp

(1) Total Cum. Production	(2) Cum. Wtr. Production	(3) Cum. Oil Production	(4) Inst. W.O.R.	(5) Oil Rec. in Hydro. P.V.	(6) Water Inj. in Hydro. P.V.
80	1	79	0.0127	0.891	0.904
160	32	128	0.632	1.445	1.805
240	73	167	1.050		
320	120	200	1.425	2.26	3.61
400	176	224	2.34		
480	222	258	1.35	2.91	5.42
560	276	284	2.08		
640	330	310	2.08	3.50	7.22
720	389	331	2.81		
800	445	355	2.34	4.00	9.04
880	499	381	2.08		
960	556	404	2.48	4.55	10.80
1040	614	426	2.64		
1120	675	445	3.21	5.01	12.65
1200	736	464	3.21		
1280	795	485	2.81	5.47	14.40
1360	859	501	4.00		
1440	925	515	4.71	5.81	16.25
1520	986	534	3.21		
1600	1052	548	4.71	6.19	18.05
1680	1117	563	4.34		
1760	1182	578	4.34	6.53	19.85
1840	1250	590	5.66		
1920	1320	600	7.00	6.77	21.70
2000	1391	609	7.90		
2080	1460	620	6.26	7.00	23.50
2160	1529	631	6.26		
2240	1601	639	9.00	7.21	25.30
2320	1671	649	7.00		
2400	1744	656	10.40	7.41	27.10

Table 13

Production History - Nine-Spot Flood 3-c

Injection Rate = 320 cc/hr S_{cw} = 23.5% μ_o = 5.592 cp

(1) Total Cum. Production	(2) Cum. Wtr. Production	(3) Cum. Oil Production	(4) Inst. W.O.R.	(5) Oil Rec. in Hydro. P.V.	(6) Water Inj. in Hydro. P.V.
80	tr.	80	0.000	0.904	0.904
160	21	139	0.356	1.56	1.805
240	59	181	0.904	2.04	2.71
320	100	220	1.050	2.48	3.61
400	144	256	1.22	2.99	4.52
480	183	297	0.95	3.35	5.42
560	230	330	1.42	3.72	6.32
640	275	365	1.285	4.12	7.22
720	325	395	1.665	4.46	8.12
800	375	425	1.665	4.80	9.04
880	423	457	1.50		
960	475	485	1.86	5.47	10.82
1040	529	511	2.08		
1120	587	533	2.64	6.02	12.65
1200	646	554	2.81		
1280	705	575	2.81	6.50	14.45
1360	765	595	3.00		
1490	827	613	3.44	6.92	16.28
1520	894	626	5.15		
1600	964	636	7.00	7.19	18.05
1680	1031	649	5.15		
1760	1100	660	6.27	7.45	19.85
1840	1170	670	7.00		
1920	1242	678	9.00	7.66	21.70
2000	1314	686	9.00	7.75	22.60

Table 14

Production History - Nine-Spot Flood 3-d

Injection Rate = 1680 cc/hr S_{cw} = 23.5% μ_o = 5.592 cp

(1) Total Cum. Production	(2) Cum. Wtr. Production	(3) Cum. Oil Production	(4) Inst. W.O.R.	(5) Oil Rec. in Hydro. P.V.	(6) Water Inj. in Hydro. P.V.
80	2	78	0.0256	0.87	0.904
160	45	115	1.16	1.30	1.805
240	101	139	2.33		
320	165	155	4.00	1.75	3.61
400	228	172	3.71		
480	288	192	3.00	2.165	5.42
560	356	204	5.66		
640	424	216	5.66	2.44	7.22
720	492	228	5.66		
800	566	234	12.35	2.64	9.04
880	630	250	4.00		
960	696	264	4.71	2.98	10.80
1040	763	277	10.42		
1120	831	289	5.66	3.26	12.65
1200	905	295	12.35		
1280	970	310	4.34	3.50	14.40
1360	1037	323	5.15		
1440	1105	335	5.66	3.78	16.25
1520	1176	344	7.90		
1600	1246	354	7.00	3.99	18.05
1680	1314	366	5.66		
1760	1379	381	4.34	4.30	19.85
1840	1448	392	6.26		
1920	1523	397	15.00	4.47	21.70
2000	1592	408	6.26		
2080	1659	421	5.15	4.75	23.50
2160	1726	434	5.15		
2240	1798	442	9.00	4.95	25.30
2320	1869	451	7.90		
2400	1941	459	9.00	5.17	27.10

Table 15

Production History - Nine-Spot Flood 3-e

Injection Rate = 2240 cc/hr S_{cw} = 23.5% μ_o = 5.592 cp

(1) Total Cum. Production	(2) Cum. Wtr. Production	(3) Cum. Oil Production	(4) Inst. W.O.R.	(5) Oil Rec. in Hydro. P.V.	(6) Water Inj. in Hydro. P.V.
80	4	76	0.0525	0.857	0.904
160	49	111	1.29	1.25	1.805
240	106	134	2.48		
320	166	154	3.00	1.74	3.61
400	237	163	7.90		
480	293	187	4.00	2.11	5.42
560	357	203	4.00		
640	424	216	5.15	2.44	7.22
720	493	227	6.26		
800	562	238	6.26	2.69	9.04
880	627	253	4.34		
960	692	268	4.34	3.02	10.80
1040	758	282	4.71		
1120	828	292	7.00	3.30	12.65
1200	901	299	10.42		
1280	968	312	5.15	3.52	14.40
1360	1036	324	5.66		
1440	1106	334	7.00	3.77	16.25
1520	1175	345	6.26		
1600	1249	351	12.35	3.96	18.05
1680	1317	363	5.66		
1760	1387	372	7.00	4.20	19.85
1840	1455	385	5.66		
1920	1530	390	15.00	4.40	21.70
2000	1601	399	7.9	4.50	22.60

Table 16

Production History - Nine-Spot Flood 3-f

Injection Rate = 1400 cc/hr S_{cw} = 23.5% μ_o = 5.592 cp

(1) Total Cum. Production	(2) Cum. Wtr. Production	(3) Cum. Oil Production	(4) Inst. W.O.R.	(5) Oil Rec. in Hydro. P.V.	(6) Water Inj. in Hydro. P.V.
80	2	78	0.0256	0.88	0.904
160	40	120	0.905	1.355	1.805
240	90	144	2.34		
320	156	164	3.00	1.85	3.61
400	217	183	3.21		
480	276	204	2.81	2.30	5.42
560	336	224	3.00		
640	402	238	4.71	2.68	7.22
720	468	252	4.71		
800	536	264	5.66	2.87	9.04
880	598	282	3.45		
960	662	298	4.00	3.37	10.80
1040	731	309	6.26		
1120	798	322	5.15	3.64	12.65
1200	866	334	5.66		
1280	932	348	4.71	3.93	14.40
1360	998	362	4.71		
1440	1069	371	7.40	4.19	16.25
1520	1137	383	5.66		
1600	1207	393	7.00	4.43	18.05
1680	1275	405	5.66		
1760	1342	418	5.15	4.72	19.85
1840	1412	428	7.00		
1920	1482	438	7.00	4.95	21.70
2000	1556	444	12.35		
2080	1625	455	6.26	5.14	23.50
2160	1696	464	7.90		
2240	1769	471	10.42	5.32	25.30
2320	1829	481	7.00		
2400	1911	489	9.00	5.52	27.10

Table 17

Production History - Nine-Spot Flood 4

Injection Rate = 1680 cc/hr S_{cw} = 23.5% μ_o = 7.607 cp

(1) Total Cum. Production	(2) Cum. Wtr. Production	(3) Cum. Oil Production	(4) Inst. W.O.R.	(5) Oil Rec. in Hydro P.V.	(6) Water Inj. in Hydro. P.V.
80	4	76	0.0526	0.858	0.904
160	55	105	1.760	1.185	1.805
240	116	124	3.21		
320	190	130	12.32	1.47	3.61
400	260	140	7.00		
480	328	152	5.66	1.715	5.42
560	403	157	15.00		
640	474	166	7.89	1.875	7.22
720	548	172	12.32		
800	625	175	25.60	1.975	9.04
880	698	182	10.45		
960	774	186	19.00	2.10	10.80
1040	848	192	12.32		
1120	923	197	15.00	2.24	12.65
1200	999	201	19.00		
1280	1075	205	19.00	2.31	14.40
1360	1151	209	19.00		
1440	1225	215	12.32	2.42	16.25
1520	1304	216	79.00		
1600	1379	221	15.00	2.49	18.05
1680	1455	225	19.00		
1760	1531	229	19.00	2.58	19.85
1840	1606	234	15.00		
1920	1682	238	19.00	2.68	21.70
2000	1761	239	79.00		
2080	1837	243	19.00	2.74	23.50
2160	1914	246	25.60		
2240	1989	251	15.00	2.83	25.30
2320	2066	254	25.60		
2400	2143	257	25.60	2.97	27.10

Table 18

Production History - Nine-Spot Flood 5

Injection Rate = 1680 cc/hr S_{cw} = 20.5% μ_o = 11.786 cp

(1) Total Cum. Production	(2) Cum. Wtr. Production	(3) Cum. Oil Production	(4) Inst. W.O.R.	(5) Oil Rec. in Hydro. P.V.	(6) Water Inj. in Hydro. P.V.
80	8	72	0.110	0.846	0.942
160	64	96	2.33	1.13	1.880
240	130	110	4.71		
320	197	123	5.15	1.45	3.77
400	274	126	25.65		
480	345	135	7.89	1.59	5.65
560	419	141	12.32		
640	495	145	19.00	1.66	7.52
720	571	149	15.00		
800	647	153	19.00	1.755	9.42
880	722	158	15.00		
960	796	164	12.30	1.930	11.30
1040	871	169	15.00		
1120	951	169		1.990	13.20
1200	1024	176	10.40		
1280	1100	180	19.00	2.12	15.05
1360	1175	185	15.00		
1440	1252	188	25.65	2.21	16.95
1520	1329	191	25.65		
1600	1405	195	19.00	2.29	18.80
1680	1480	200	15.00		
1760	1555	205	15.00	2.41	20.70
1840	1633	207	39.00		
1920	1710	210	25.65	2.47	22.60
2000	1788	212	39.00		
2080	1866	214	39.00	2.52	24.40
2160	1944	216	39.00		
2240	2020	220	19.00	2.59	26.40
2320	2098	222	39.00		
2400	2176	224	39.00	2.64	28.20

Table 19

Production History - Nine-Spot Flood 6

Injection Rate = 1680 cc/hr S_{cw} = 23.8% μ_o = 1.595 cp*

(1) Total Cum. Production	(2) Cum. Wtr. Production	(3) Cum. Oil Production	(4) Inst. W.O.R.	(5) Oil Rec. in Hydro. P.V.	(6) Water Inj. in Hydro. P.V.
80	0	80	0.000	0.9825	0.9825
160	24	136	0.429	1.67	1.963
240	66	174	1.105		
320	114	206	1.50	2.53	3.93
400	168	232	2.08		
480	219	261	1.76	3.20	5.89
560	273	287	2.08		
640	328	312	2.20	3.83	7.85
720	400	320	9.00		
800	464	336	4.00	4.125	9.825
880	525	355	3.21		
960	589	371	4.00	4.55	11.80
1040	654	386	4.33		
1120	721	399	5.15	4.88	13.75
1200	791	409	7.00		
1280	857	423	4.72	5.20	15.75
1360	924	436	5.15		
1440	994	446	7.00	5.47	17.65
1520	1065	456	7.00		
1600	1137	463	10.40	5.68	19.65
1680	1208	472	7.89		
1760	1280	480	9.00	5.89	21.60
1840	1355	485	15.00		
1920	1428	492	10.40	6.03	23.60
2000	1503	497	15.00		
2080	1577	503	12.32	6.18	25.60
2160	1651	509	12.32		
2240	1725	515	12.32	6.31	27.50
2320	1802	518	25.65		
2400	1876	524	12.32	6.43	29.50

* μ_w = 3.185 cp

Table 20

Nine-Spot Flood 1-a: Calculation of Areal Sweep Efficiency (Eas) and Displacement Efficiency (Ed)

Injection Rate = 560 cc/hr S_{cw} = 19.69% C = 1.679

(1) Water Injected in Hydro. P.V.	(2) Area Measured cm^2	(3) Eas. Area/Unit Area Fraction	(4) Es Cum. Oil Prod. in Hydro. P.V.	(5) Ed Col. 4/Col. 3
0.932	315	0.763	0.932	
4.66	2110	5.10	3.37	0.660
9.32	2698	6.53	5.37	0.821
14.00	2880	6.97	6.24	0.891
28.00	3000	7.26	7.05	0.970

Table 21

Nine-Spot Flood 1-b: Calculation of Areal Sweep Efficiency (Eas) and Displacement Efficiency (Ed)

Injection Rate = 1120 cc/hr S_{cw} = 17.25% C = 1.679

(1) Water Injected in Hydro. P.V.	(2) Area Measured cm^2	(3) Eas Area/Unit Area Fraction	(4) Es Cum. Oil Prod. in Hydro. P.V.	(5) Ed Col. 4/Col. 3
0.9025	296.5	0.718	0.9025	
4.013	1820	4.41	3.13	0.710
9.025	2485	6.02	4.89	0.815
13.55	2680	6.49	5.94	0.918
18.09	2830	6.85	6.57	0.962
27.10	2960	7.16	7.21	1.000

Table 22

Nine-Spot Flood 1-c: Calculation of Areal Sweep Efficiency (Eas), Displacement Efficiency (Ed) and Mobility Ratio (M).

Injection Rate = 1680 cc/hr S_{cw} = 15.07% C = 1.679

(1) Water Inj. Hydro. P.V.	(2) Area Measured cm^2	(3) Eas Area/Unit Area Fraction	(4) Es Cum. Oil Prod. in Hydro. P.V.	(5) Ed Col. 4/Col. 3	(6) $\overline{S}_w$*	(7) K_{ro}	(8) K_{rw}	(9) M $M = \frac{K_{rw}\mu_o}{K_{ro}\mu_w}$
0.879	420	1.018	0.879	0.865	0.886	0.48	0.495	1.732
1.760	855	2.07	1.605	0.726	0.768	0.48	0.350	1.225
2.64	1229	2.98	2.15	0.725	0.767	0.48	0.350	1.225
4.40	1745	4.22	3.04	0.722	0.765	0.48	0.350	1.225
8.80	2550	6.17	4.67	0.756	0.795	0.48	0.380	1.330
13.20	2839	6.86	5.83	0.850	0.873	0.48	0.480	1.679
17.60	3030	7.34	6.59	0.901	0.917	0.48	0.565	1.975
26.40	3240	7.84	7.56	0.956	0.964	0.48	0.740	2.585

* $\overline{S}_w = S_{cw} + (1 - S_{cw})Ed$

Table 23

Nine-Spot Flood 1-d: Calculation of Areal Sweep Efficiency (Eas) and Displacement Efficiency (Ed)

Injection Rate = 2240 cc/hr S_{cw} = 18.82% C = 1.679

(1) Water Injected in Hydro. P.V.	(2) Area Measured cm^2	(3) Eas Area/Unit Area Fraction	(4) Es Cum. Oil Prod. in Hydro. P.V.	(5) Ed Col. 4/Col. 3
0.921	351.5	0.85	0.921	
1.845	612	1.48	1.50	
2.77	1020	2.47	1.91	0.776
4.61	1585	3.84	2.68	0.700
9.21	2240	5.43	4.19	0.775
13.84	2575	6.24	5.22	0.839
18.45	2752	6.67	5.91	0.887
27.70	2939	7.11	6.72	0.945

Table 24

Nine-Spot Flood 2: Calculation of Areal Sweep Efficiency (Eas), Displacement Efficiency (Ed) and Mobility Ratio (M).

Injection Rate = 1120 cc/hr $\quad$ S_{cw} = 23.5% $\quad$ C = 3.520

(1) Water Inj. Hydro. P.V.	(2) Area Measured cm^2	(3) Eas Area/Unit Area Fraction	(4) Es Cum. Oil Prod. in Hydro. P.V.	(5) Ed Col. 4/Col. 3	(6) $\bar{S}_w$*	(7) K_{ro}	(8) K_{rw}	(9) M $M = \frac{K_{rw}\mu_o}{K_{ro}\mu_w}$
0.904	435	1.05	0.925	0.860	0.895	0.39	0.515	4.64
1.804	839	2.03	1.55	0.764	0.819	0.39	0.405	3.655
2.71	1160	2.81	1.92	0.685	0.759	0.39	0.340	3.18
4.52	1630	3.95	2.64	0.671	0.748	0.39	0.330	2.98
9.25	2465	5.97	4.10	0.689	0.762	0.39	0.345	3.11
13.55	2930	7.10	5.25	0.744	0.803	0.39	0.390	3.52
18.65	3145	7.62	6.24	0.822	0.864	0.39	0.462	4.16
27.10	3475	8.40	7.62	0.907	0.929	0.39	0.600	5.42

* $\bar{S}_w = S_{cw} + (1-S_{cw})Ed$

Table 25

Nine-Spot Flood 3-a: Calculation of Areal Sweep Efficiency (Eas) and Displacement Efficiency (Ed)

Injection Rate = 1120 cc/hr S_{cw} = 23.5% C = 6.265

(1) Water Injected in Hydro. P.V.	(2) Area Measured cm^2	(3) Eas Area/Unit Area Fraction	(4) Es Cum. Oil Prod. in Hydro. P.V.	(5) Ed Col. 4/Col. 3
0.904	444	1.075	0.892	0.832
1.805	678	1.64	1.350	0.829
2.71	895	2.165	1.66	0.768
4.52	1198	2.90	2.15	0.745
9.04	1870	4.53	3.14	0.695
13.55	2500	6.05	4.07	0.675
22.60	3160	7.65	5.68	0.745

Table 26

Nine-Spot Flood 3-b: Calculation of Areal Sweep Efficiency (Eas) and Displacement Efficiency (Ed)

Injection Rate = 560 cc/hr S_{cw} = 23.5%   C = 6.265

(1) Water Injected in Hydro. P.V.	(2) Area Measured cm^2	(3) Eas Area/Unit Area Fraction	(4) Es Cum. Oil Prod. in Hydro. P.V.	(5) Ed Col. 4/Col. 3
0.904	566	1.37	0.904	0.653
1.805	971	2.35	1.445	0.587
2.71	1253	3.03	1.885	0.623

Table 27

Nine-Spot Flood 3-c: Calculation of Areal Sweep Efficiency (Eas) and Displacement Efficiency (Ed)

Injection Rate = 320 cc/hr S_{cw} = 23.5%   C = 6.265

(1) Water Injected in Hydro. P.V.	(2) Area Measured cm^2	(3) Eas Area/Unit Area Fraction	(4) Es Cum. Oil Prod. in Hydro. P.V.	(5) Ed Col. 4/Col. 3
0.904	684	1.655	0.904	0.546
1.805	1216	2.94	1.56	0.535
2.71	1680	4.07	2.04	0.503
4.52	2350	5.69	2.99	0.510
9.04	3050	7.39	4.80	0.651
13.55	3441	8.33	6.25	0.752
22.60	3680	8.91	7.75	0.873

Table 28

Nine-Spot Flood 3-d: Calculation of Areal Sweep Efficiency (Eas),

Displacement Efficiency (Ed) and Mobility Ratio (M).

Injection Rate = 1680 cc/hr | S_{cw} = 23.5% | C = 6.265

(1) Water Inj. Hydro. P.V.	(2) Area Measured cm^2	(3) Eas Area/Unit Area Fraction	(4) Es Cum. Oil Prod. in Hydro. P.V.	(5) Ed Col. 4/Col. 3	(6) $\overline{S}_w$ *	(7) K_{ro}	(8) K_{rw}	(9) M $M = \frac{K_{rw}\mu_o}{K_{ro}\mu_w}$
0.904	484	1.17	0.87	0.754	0.811	0.39	0.40	6.42
1.805	688	1.67	1.30	0.780	0.831	0.39	0.42	6.75
2.71	844	2.04	1.57	0.770	0.825	0.39	0.415	6.67
4.52	1045	2.53	1.94	0.768	0.823	0.39	0.413	6.64
9.04	1485	3.59	2.64	0.736	0.799	0.39	0.385	6.18
13.52	2015	4.88	3.33	0.685	0.759	0.39	0.34	5.47
18.05	2459	5.95	3.99	0.673	0.750	0.39	0.33	5.30
27.10	3020	7.31	5.17	0.710	0.779	0.39	0.36	5.78

* $\overline{S}_w = S_{cw} + (1-S_{cw})Ed$

Table 29

Nine-Spot Flood 3-e: Calculation of Areal Sweep Efficiency (Eas) and Displacement Efficiency (Ed)

(1) Water Injected in Hydro. P.V.	(2) Area Measured cm^2	(3) Eas Area/Unit Area Fraction	(4) Es Cum. Oil Prod. in Hydro. P.V.	(5) Ed Col. 4/Col. 3
4.52	1130	2.76	1.84	0.675
9.04	1744	4.22	2.69	0.638
13.52	2135	5.17	3.375	0.655
18.05	2425	5.87	3.96	0.675

Table 30

Nine-Spot Flood 3-f: Calculation of Areal Sweep Efficiency (Eas) and Displacement Efficiency (Ed)

Injection Rate = 1400 cc/hr S_{cw} = 23.5% C = 6.265

(1) Water Injected in Hydro. P.V.	(2) Area Measured cm^2	(3) Eas Area/Unit Area Fraction	(4) Es Cum. Oil Prod. in Hydro. P.V.	(5) Ed Col. 4/Col. 3
0.904	596	1.28	0.88	0.612
1.805	828	1.78	1.355	0.675
2.71	953	2.04	1.625	0.706
4.52	1238	2.65	2.062	0.691
9.04	1809	3.87	2.87	0.682
13.52	2365	5.06	3.77	0.660
18.05	2755	5.90	4.43	0.666
27.10	3200	6.85	5.52	0.715

Table 31

Nine-Spot Flood 4: Calculation of Areal Sweep Efficiency (Eas), Displacement Efficiency (Ed) and Mobility Ratio (M).

(1) Water Inj. Hydro. P.V.	(2) Area Measured cm^2	(3) Eas Area/Unit Area Fraction	(4) Es Cum. Oil Prod. in Hydro. P.V.	(5) Ed Col. 4/Col. 3	(6) $\bar{S}_w$*	(7) K_{ro}	(8) K_{rw}	(9) M $M = \frac{K_{rw}\mu_o}{K_{ro}\mu_w}$
0.904	568	1.38	0.858	0.625	0.713	0.39	0.295	6.05
1.805	725	1.76	1.185	0.678	0.753	0.39	0.34	6.97
4.52	952	2.30	1.580	0.686	0.760	0.39	0.34	6.97
9.04	1170	2.83	1.975	0.695	0.767	0.39	0.345	7.08
22.50	1300	3.15	2.70	0.860	0.893	0.39	0.51	10.45

* $\bar{S}_w = S_{cw} + (1-S_{cw})Ed$

Table 32

Nine-Spot Flood 5: Calculation of Areal Sweep Efficiency (Eas), Displacement Efficiency (Ed) and Mobility Ratio (M).

Injection Rate = 1680 cc/hr $\quad$ S_{cw} = 20.5% $\quad$ C = 12.405

(1) Water Inj. Hydro. P.V.	(2) Area Measured cm^2	(3) Eas Area/Unit Area Fraction	(4) Es Cum. Oil Prod. in Hydro. P.V.	(5) Ed Col. 4/Col. 3	(6) $\overline{S}_w$*	(7) K_{ro}	(8) K_{rw}	(9) M $M = \frac{K_{rw}\mu_o}{K_{ro}\mu_w}$
0.942	510	1.24	0.846	0.685	0.745	0.42	0.33	9.75
1.880	631	1.53	1.13	0.740	0.793	0.42	0.38	11.20
4.70	842	2.04	1.482	0.726	0.782	0.42	0.37	10.92
9.42	1015	2.46	1.80	0.732	0.787	0.42	0.37	10.92
28.20	1550	3.75	2.64	0.703	0.765	0.42	0.35	10.35

* $\overline{S}_w = S_{cw} + (1-S_{cw})Ed$

Table 33

Nine-Spot Flood 6: Calculation of Areal Sweep Efficiency (Eas), Displacement Efficiency (Ed) and Mobility Ratio (M).

Injection Rate = 1680 cc/hr $\quad S_{cw}$ = 23.80% $\quad$ C = 0.5007

(1) Water Inj. Hydro. P.V.	(2) Area Measured cm^2	(3) Eas Area/Unit Area Fraction	(4) Es Cum. Oil Prod. in Hydro. P.V.	(5) Ed Col. 4/Col. 3	(6) $\overline{S}_w$ *	(7) K_{ro}	(8) K_{rw}	(9) M $M = \frac{K_{rw}\mu_o}{K_{ro}\mu_w}$
.9825	348	0.84	0.9825	--	--	0.44	--	--
1.963	632	1.53	1.67	--	--	0.44	--	--
2.95	854	2.06	2.14	--	--	0.44	--	--
4.92	1270	3.08	2.85	0.925	0.943	0.44	0.66	0.75
9.825	1998	4.84	4.125	0.850	0.884	0.44	0.50	0.568
14.72	2295	5.56	5.02	0.901	0.923	0.44	0.595	0.675
29.50	2695	6.52	6.425	0.986	0.988	0.44	0.900	1.022

* $\overline{S}_w = S_{cw} + (1-S_{cw})Ed$

Table 34

Calculation of Areal Sweep Efficiency (Eas) and Mobility Ratio (M)

at Breakthrough for all Floods

Flood No.	Hydro. P.V. of Unit Area cc	Oil Rec. to B.T. cc		Ed*		Eas** Fraction		M***
		Direct Wells	Diagonal Wells	Direct Wells	Diagonal Wells	Direct Wells	Diagonal Wells	
1-c	91.0	89.6	154	0.865	0.726	1.14	2.33	1.622
2	88.6	74.6	146	0.860	0.764	0.980	2.16	3.833
3-d	88.6	61.6	120.5	0.754	0.780	0.922	1.74	6.150
4	88.6	56	84	0.625	0.678	1.01	1.40	7.504
5	85.0	46.7	63	0.685	0.740	0.80	1.001	10.63
6	81.5	72.5	117	0.925	0.925	0.962	1.552	0.75

* Ed - From previous calculations

** Eas - calculated from Oil Rec. = Ed x Eas x P.V. (Unit Area)

*** M - calculated as outlined previously

Table 35

Nine-Spot Flood 1-c: Calculation of Q/Q_{BT}

$C = 1.679$

(1) Eas Measured Fraction	(2) Q Cum. Water Injected (cc)	(3) Q/Q_{BT} Direct	(4) Q/Q_{BT} Diagonal
1.018	80	0.8925	0.46
2.07	160	1.685	0.92
2.98	240	2.678	1.38
4.22	400	4.463	2.30
6.17	800	8.925	4.60
6.86	1200	13.400	6.90
7.34	1600	16.850	9.20
7.84	2400	26.775	13.80

Volume Injected Before Breakthrough: (ie Q_{BT})

1. Direct offset wells - 89.6 cc.
2. Diagonal offset wells - 174 cc.

Table 36

Nine-Spot Flood 2: Calculation of Q/Q_{BT}

$C = 3.52$

(1) Eas Measured Fraction	(2) Q Cum. Water Injected (cc)	(3) Q/Q_{BT} Direct	(4) Q/Q_{BT} Diagonal
1.05	80	1.072	0.445
2.03	160	2.144	0.89
2.81	240	3.216	1.34
3.94	400	5.360	2.23
5.97	800	10.720	4.45
7.10	1200	16.100	6.69
7.62	1600	21.440	8.90
8.40	2400	32.160	13.35

Volume Injected Before Breakthrough (ie Q_{BT})

1. Direct offset wells - 74.6 cc.
2. Diagonal offset wells - 179.5 cc.

Table 37

Nine-Spot Flood 3-d: Calculation of Q/Q_{BT}

C = 6.265

(1) Eas Measured Fraction	(2) Q Cum. Water Injected (cc)	(3) Q/Q_{BT} Direct	(4) Q/Q_{BT} Diagonal
1.17	80	1.30	0.623
1.67	160	2.60	1.25
2.04	240	3.90	1.87
2.53	400	6.50	3.12
3.59	800	13.00	6.23
4.88	1200	19.50	9.35
5.95	1600	26.00	12.46
7.31	2400	39.00	18.69

Volume Injected Before Breakthrough (ie Q_{BT})

1. Direct offset wells - 61.6 cc.
2. Diagonal offset wells - 128.5 cc.

Table 38

Nine-Spot Flood 4: Calculation of Q/Q_{BT}

C = 8.007

(1) Eas Measured Fraction	(2) Q Cum. Water Injected (cc)	(3) Q/Q_{BT} Direct	(4) Q/Q_{BT} Diagonal
1.38	80	1.43	0.816
1.755	160	2.86	1.632
2.30	400	7.15	4.08
2.83	800	14.30	8.16
3.15	2000	35.70	20.40

Volume Injected Before Breakthrough (ie Q_{BT})

1. Direct offset wells - 56 cc.
2. Diagonal offset wells - 98 cc.

Table 39

Nine-Spot Flood 5: Calculation of Q/Q_{BT}

$C = 12.405$

(1) Eas Measured Fraction	(2) Q Cum. Water Injected (cc)	(3) Q/Q_{BT} Direct	(4) Q/Q_{BT} Diagonal
1.235	80	1.715	1.225
1.53	160	3.43	2.45
2.04	400	8.57	6.12
2.46	800	17.15	12.25
3.75	2400	51.50	36.70

Volume Injected Before Breakthrough (ie Q_{BT})

1. Direct offset wells - 46.7 cc.
2. Diagonal offset wells - 65.4 cc.

Table 40

Nine-Spot Flood 6: Calculation of Q/Q_{BT}

$C = 0.5007$

(1) Eas Measured Fraction	(2) Q Cum. Water Injected (cc)	(3) Q/Q_{BT} Direct	(4) Q/Q_{BT} Diagonal
0.84	80	1.12	0.665
1.53	160	2.21	1.33
2.06	240	3.31	2.00
3.08	400	5.52	3.34
4.04	800	11.20	6.65
5.56	1200	16.55	10.00
6.52	2400	33.10	20.00

Volume Injected Before Breakthrough (ie Q_{BT})

1. Direct offset wells - 72.5 cc.
2. Diagonal offset wells - 120.0 cc.

Table 41

Miscellaneous Data

Flood No.	Injection Rate cc/hr	Model No.	S_{cw}%	Unit Area Hydrocarbon Pore Volume cc	μ_o cp	μ_w cp
1	320	II	20.76	84.6	1.595	0.95
1-a	560	II	19.69	85.8	1.595	0.95
1-b	1120	II	17.25	88.6	1.595	0.95
1-c	1680	II	15.07	91.0	1.595	0.95
1-d	2240	II	18.82	86.8	1.595	0.95
1-e	2800	II	20.25	85.2	1.595	0.95
2	1120	I	23.50	88.6	3.342	0.95
3-a	1120	I	23.50	88.6	5.592	0.95
3-b	560	I	23.50	88.6	5.592	0.95
3-c	320	I	23.50	88.6	5.592	0.95
3-d	1680	I	23.50	88.6	5.592	0.95
3-e	2240	I	23.50	88.6	5.592	0.95
3-f	1400	I	23.50	88.6	5.592	0.95
4	1680	I	23.50	88.6	7.607	0.95
5	1680	II	20.50	85.0	11.786	0.95
6	1680	II	23.80	81.5	1.595	3.185

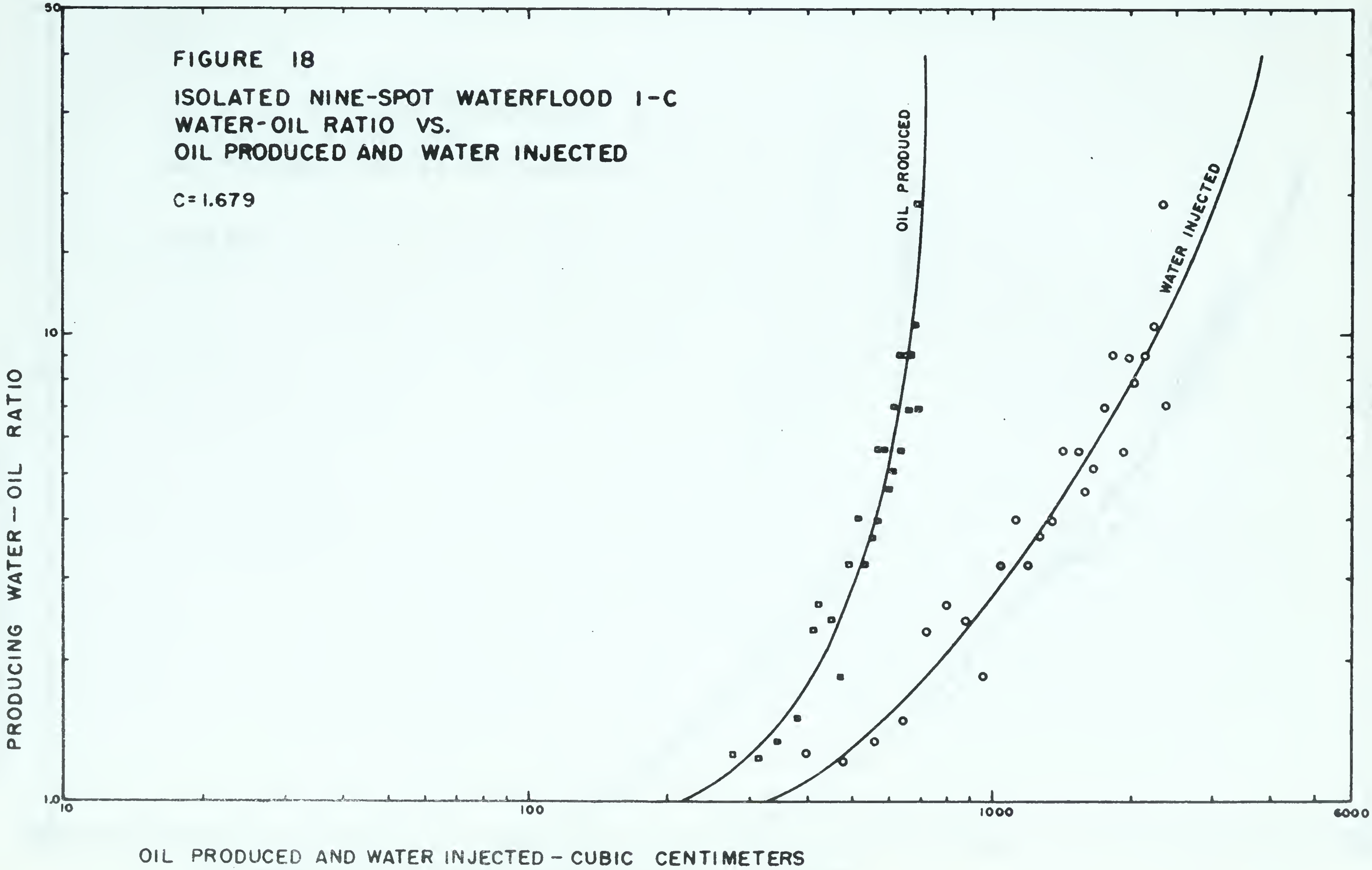

FIGURE 18

ISOLATED NINE-SPOT WATERFLOOD I-C
WATER-OIL RATIO VS.
OIL PRODUCED AND WATER INJECTED

C= 1.679

FIGURE 14

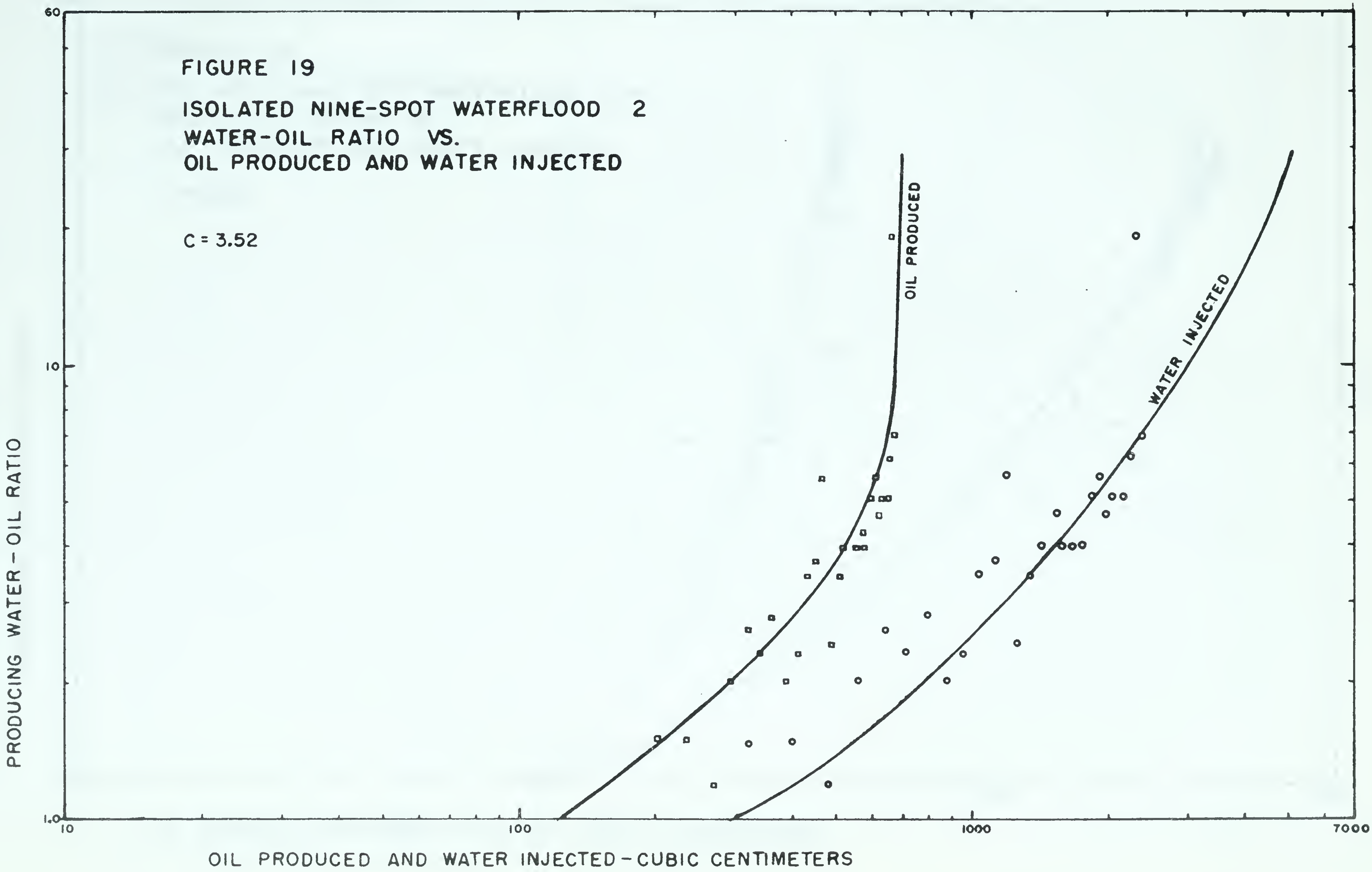
FIGURE 19
ISOLATED NINE-SPOT WATERFLOOD 2
WATER-OIL RATIO VS.
OIL PRODUCED AND WATER INJECTED
C = 3.52
OIL PRODUCED
WATER INJECTED
60
10
1.0
10
100
1000
7000
PRODUCING WATER - OIL RATIO
OIL PRODUCED AND WATER INJECTED - CUBIC CENTIMETERS

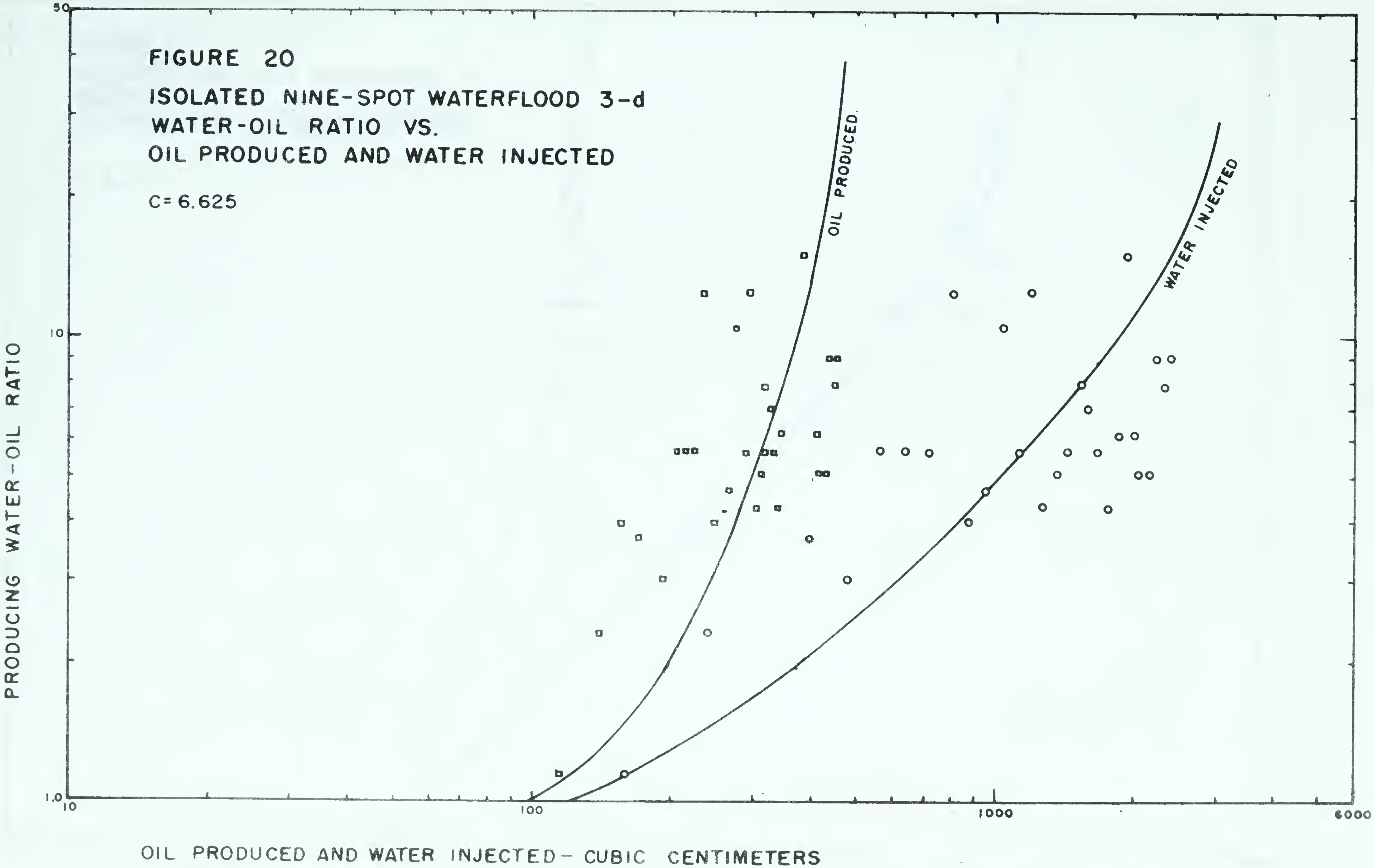

FIGURE 20

ISOLATED NINE-SPOT WATERFLOOD 3-d
WATER-OIL RATIO VS.
OIL PRODUCED AND WATER INJECTED

C= 6.625

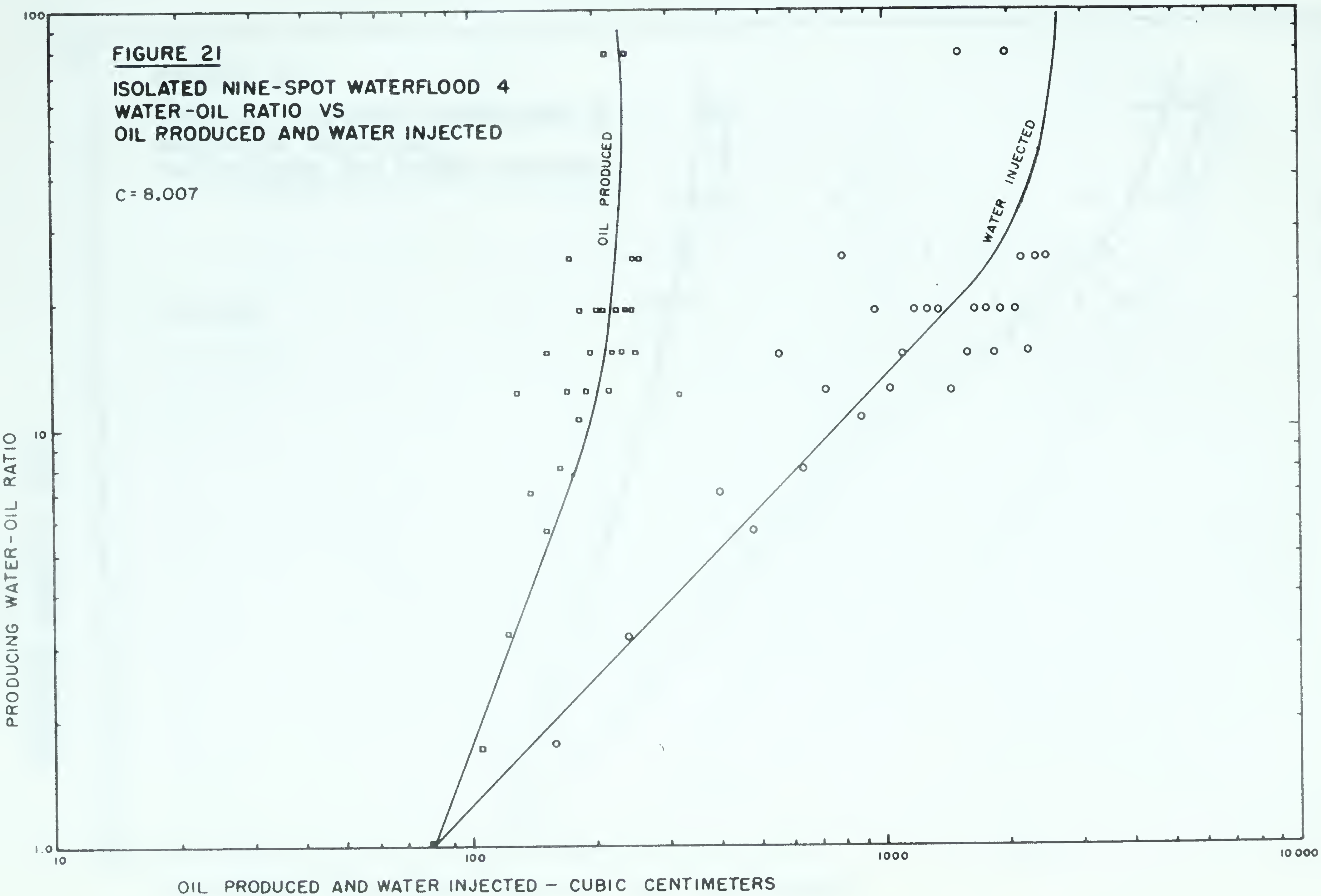

FIGURE 21

ISOLATED NINE-SPOT WATERFLOOD 4
WATER-OIL RATIO VS
OIL PRODUCED AND WATER INJECTED

C = 8.007

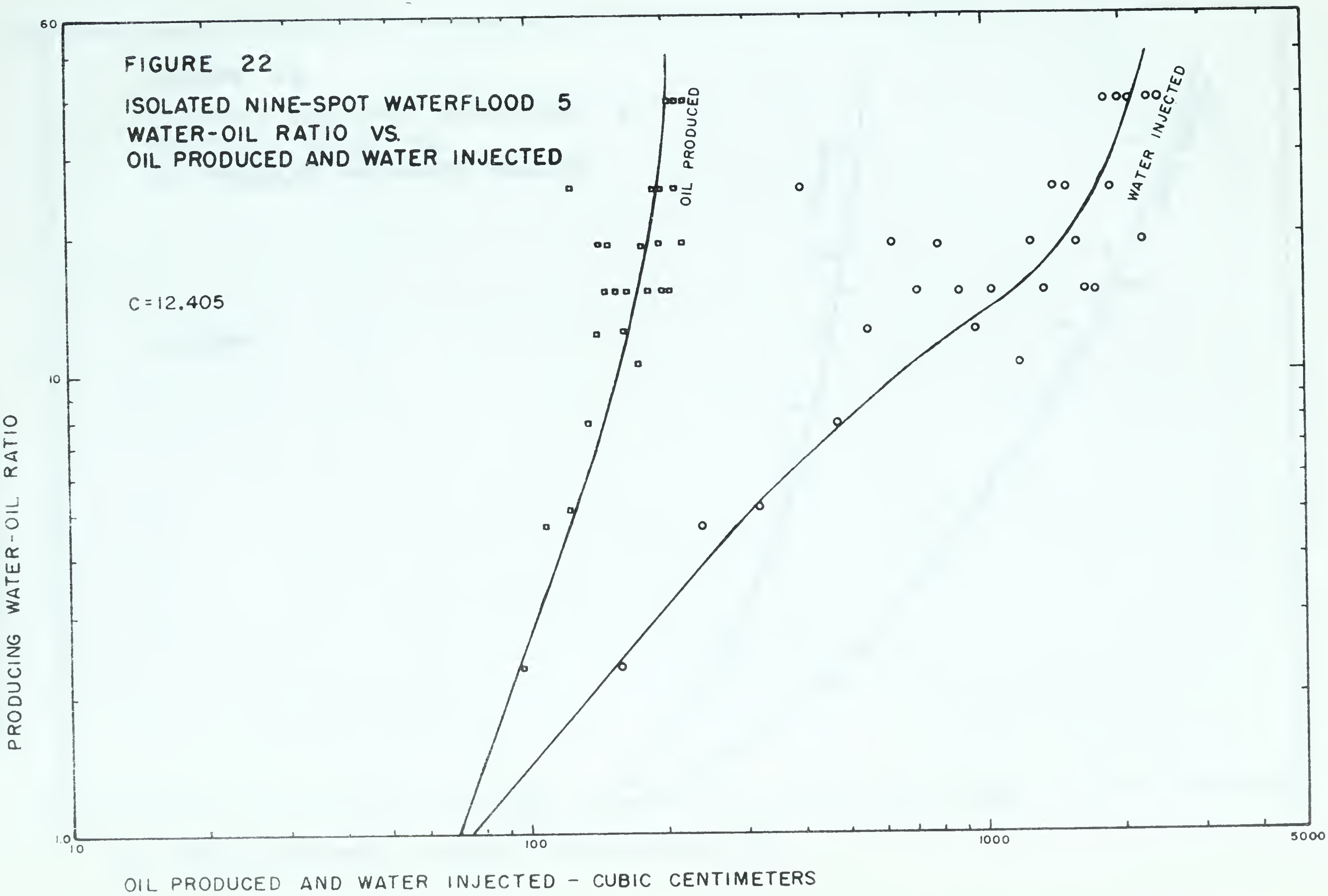

FIGURE 22

ISOLATED NINE-SPOT WATERFLOOD 5
WATER-OIL RATIO VS.
OIL PRODUCED AND WATER INJECTED

C = 12.405

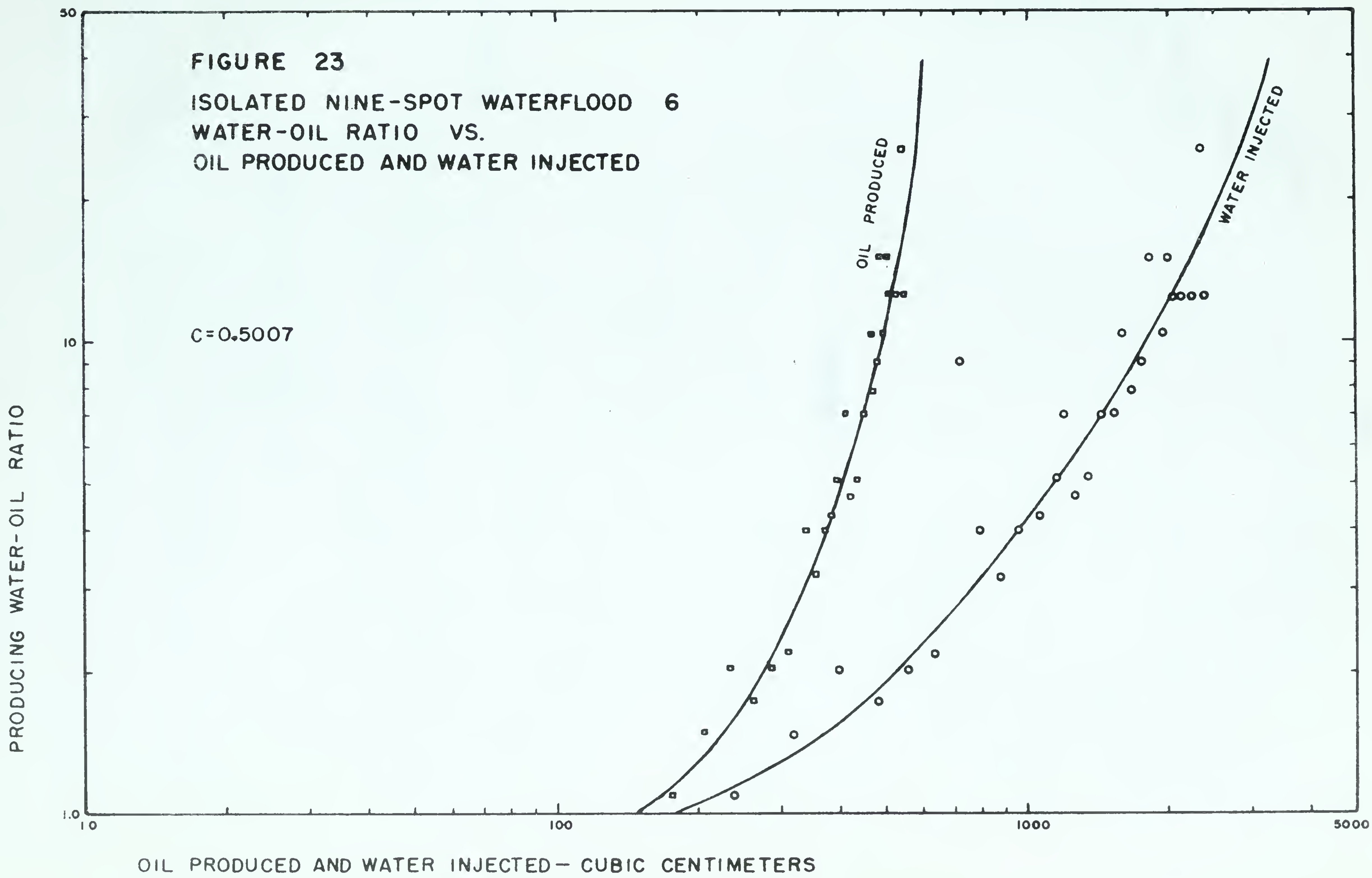
FIGURE 23
ISOLATED NINE-SPOT WATERFLOOD 6
WATER-OIL RATIO VS.
OIL PRODUCED AND WATER INJECTED
C=0.5007
OIL PRODUCED
WATER INJECTED
50
10
1.0
10
100
1000
5000
PRODUCING WATER-OIL RATIO
OIL PRODUCED AND WATER INJECTED— CUBIC CENTIMETERS

APPENDIX B

DERIVATION OF TWO-DIMENSIONAL SCALING COEFFICIENT

The following equation, set forth by Rapoport,[22] describes the displacement of oil by water in a three dimensional system. This equation is of general applicability with respect to any three dimensional transient flow process involving two incompressible fluids, the exact nature of which is defined by the prevailing boundary conditions. It accounts explicitly for the frictional, gravitational and capillary forces and can be classified as the complete displacement equation:

$$(1) \qquad \phi \frac{\partial S_w}{\partial t} + \frac{df_w}{dS_w}\left(q_x \frac{\partial S_w}{\partial x} + q_y \frac{\partial S_w}{\partial y} + q_z \frac{\partial S_w}{\partial z}\right) - \frac{K}{\mu_o}\left[\frac{\partial}{\partial x}\left(K_{ro} f_w \frac{dP_c}{dS_w} \cdot \frac{\partial S_w}{\partial x}\right) + \frac{\partial}{\partial y}\left(K_{ro} f_w \frac{dP_c}{dS_w} \cdot \frac{\partial S_w}{\partial y}\right) + \frac{\partial}{\partial z}\left(K_{ro} f_w \frac{dP_c}{dS_w} \cdot \frac{\partial S_w}{\partial z}\right)\right] - \frac{K\, g\Delta\rho}{\mu_o} \frac{d\left(K_{ro} f_w\right)}{dS_w} \cdot \frac{\partial S_w}{\partial z} = 0$$

Accepting the above equation and neglecting the effect of gravity it reduces to equation (2):

$$(2) \qquad \phi \frac{\partial S_w}{\partial t} + \frac{df_w}{dS_w}\left(q_x \frac{\partial S_w}{\partial x} + q_y \frac{\partial S_w}{\partial y}\right) - \frac{K}{\mu_o}\left[\frac{\partial}{\partial x}\left(K_{ro} f_w \frac{dP_c}{dS_w} \cdot \frac{\partial S_w}{\partial x}\right) + \frac{\partial}{\partial y}\left(K_{ro} f_w \frac{dP_c}{dS_w} \cdot \frac{\partial S_w}{\partial x}\right)\right] = 0$$

Equation (2) represents complete flooding conditions in which capillary pressure is accounted for.

To obtain the dimensionless form of equation (2) the injection rate q will be considered a constant. Therefore only two variables remain to be normalized (ie: length and time). Defining

$X = \frac{x}{L}$ and $Y = \frac{y}{L}$ - where X and Y represent distance expressed as a function of total length and width of the system.

$T = \frac{tq}{L^2 \phi}$ - where T is dimensionless time co-ordinate or cumulative injection in number of pore volumes.

Taking derivative of the above expression produces:

$$\frac{\partial S_w}{\partial X} = L\frac{\partial S_w}{\partial x} \; ; \; \frac{\partial S_w}{\partial Y} = L\frac{\partial S_w}{\partial y} \text{ and } \frac{\partial S_w}{\partial T} = \frac{L^2\phi}{q} \cdot \frac{\partial S_w}{\partial t}$$

substituting into equation (2) and using $c\mu_w$ for μ_o

$$\text{(3)} \qquad \frac{q}{L^2\phi} \cdot \phi \frac{\partial S_w}{\partial T} + \frac{1}{L}\frac{df_w}{dS_w}\left(q_x\frac{\partial S_w}{\partial X} + q_y\frac{\partial S_w}{\partial Y}\right) - \frac{K}{c\mu_w} \cdot \frac{1}{L^2}$$

$$\left[\frac{\partial}{\partial X}\left(K_{ro} f_w \frac{dP_c}{dS_w} \cdot \frac{\partial S_w}{\partial X}\right) + \frac{\partial}{\partial Y}\left(K_{ro} f_w \frac{dP_c}{dS_w} \cdot \frac{\partial S_w}{\partial Y}\right)\right] = 0$$

Define (a) $\frac{q_x}{q/L} = Q_x$ and (b) $\frac{q_y}{q/L} = Q_y$ as velocity distribution functions (1) in the x and y direction respectively.

Where q - rate of water injection per unit sand thickness (cc/cm/sec)

q_x, q_y - rate of flow per unit c.s.a. ($cc/cm^2/sec$)

L - principal dimension - size of nine-spot (cm)

Now introducing Leverett's J-function where

$$P_c = \frac{J(S_w)\,\sigma_{ow}\cos\theta}{\sqrt{K/\ \phi}}$$ and taking derivative w.r.t. S_w get:

(c) $$\frac{dP_c}{dS_w} = \frac{dJ(S_w)}{dS_w} \cdot \frac{\sigma_{ow}\cos\theta\sqrt{\phi}}{\sqrt{K}}$$

Making the appropriate substitutions of (a), (b) and (c) into equation (3) results in:

(4) $$\frac{\partial S_w}{\partial T} + \frac{df_w}{dS_w}\left(Q_x\frac{\partial S_w}{\partial X} + Q_y\frac{\partial S_w}{\partial Y}\right) - \frac{1}{C} \cdot \frac{\sigma_{ow}\cos\theta\sqrt{K\phi}}{q\,\mu_w} \cdot$$

$$\left[\frac{\partial}{\partial X}\left(K_{ro}f_w\,\frac{dJ(S_w)}{dS_w} \cdot \frac{\partial S_w}{\partial X}\right) + \frac{\partial}{\partial Y}\left(K_{ro}f_w\,\frac{dJ(S_w)}{dS_w} \cdot \frac{\partial S_w}{\partial Y}\right)\right] = 0$$

Equation (4) leads to the coefficient of $\dfrac{q\,\mu_w}{\sigma_{ow}\cos\theta\sqrt{K\,\phi}}$ which can be used to correlate systems having only the same viscosity ratio, initial saturation distribution and pore size distribution. Thus this coefficient is known as the "capillary pressure coefficient" or scaling coefficient and was denoted by "C_2" (proposed by Rapoport[23]).

If the appropriate units are used for "C_2" it is a dimensionless coefficient. ie:

q - cc/cm/sec (cm^2/sec)

μ_w - cp (gram/cm-sec)

σ_{ow} - dyne/cm (gram-cm/sec^2-cm)

K - darcy (cm^2)

NOMENCLATURE

Subscripts o and w pertain to oil and water, respectively.

S_w	- water saturation - dimensionless fraction (1)
x,y,z	- spatial co-ordinates (cm)
t	- time (sec)
L	- principal dimension (cm)
$Y = \frac{y}{L}$ $X = \frac{x}{L}$	- dimensionless space co-ordinates (1)
q	- rate of water injection per unit sand thickness (cc/cm/sec)
ϕ	- porosity, dimensionless fraction (1)
K	- absolute permeability (darcies)
σ	- water-oil interfacial tension (dyne/cm)
μ_o, μ_w	- viscosity (cp)
c	- oil-water viscosity ratio (1)
q_x, q_y	- rate of flow per unit c.s.a. ($cc/cm^2/sec$)
$Q_x, Q_y = \frac{q_{xy}}{q/L}$	- velocity distribution function (1)
K_{ro}, K_{rw}	- relative permeabilities dimensionless function of saturation (1)
T	- dimensionless time (1)
$F_w = \left[1 + \frac{K_{ro}\mu_w}{K_{rw}\mu_o}\right]^{-1}$	- dimensionless function of saturation
$J(S_w) = \frac{P_c}{\sigma}\left(\frac{K}{\phi}\right)^{1/2}$	- capillary retention function, dimensionless function of saturation

Θ	- water-oil-solid contact angle, dimensionless (1)
P_c	- capillary pressure, function of saturation (atm)
$\Delta\rho$	- density difference between oil and water (gm/cm^3)
K_o, K_w	- effective permeability (darcy)
E_{as}	- areal sweep efficiency, dimensionless (1)
E_d	- displacement efficiency, dimensionless (1)
E_s	- total sweep efficiency, dimensionless (1)